Aust. J. Phys., 1979, **32**, 585–628

Low Temperature Transport Properties of the Group V Semimetals*

J-P. Issi

Laboratoire de Physico-chimie et de Physique de l'État Solide, Université Catholique de Louvain, 1 Place Croix du Sud, B-1348 Louvain-la-Neuve, Belgium.

Abstract

The group V semimetals are first introduced by comparing their particular band structure with the more familiar typical metals or semiconductors. Recent results on the electrical resistivity, thermal conductivity and thermopower of bismuth, antimony and arsenic are reviewed, with particular emphasis on measurements performed at low and ultralow temperatures. The data are analysed in terms of the peculiar features of the electron and phonon scattering, and reference is made to the band structure and rhombohedral symmetry. Recent improvements in the interpretation of the results are discussed.

1. Introduction

Solid state physics owes to semimetals, and especially to bismuth, many of the sophisticated techniques currently used nowadays to probe the Fermi surface and the band structure of crystalline solids. Most of the sharpest tools in the armoury of experimentalists, such as quantum oscillatory techniques (de Haas van Alphen, Shubnikov de Haas, ...), were indeed discovered on bismuth. This is no accident, since its particular properties facilitate the observation of such effects. In 1821, Seebeck discovered his effect on a bismuth–antimony thermocouple. This was only the beginning of a long chain of exciting discoveries named after their authors—Hall, Ettingshausen and Nernst—which constitute the essentials of what we nowadays classify under the heading of transport effects. Despite the enormous amount of experimental work which was subsequently performed on bismuth, and to a lesser extent on antimony, however, the elementary transport properties such as the electrical and thermal conductivities and thermopower have not yet been correctly interpreted, and the scattering mechanisms in these materials still remain a challenge to our understanding.

Only recently was it realized that research on semimetals held something more than the excitement of the discovery of spectacular effects, and that time-consuming systematic experimental measurements, associated with some tedious algebra, might prove rewarding in yielding valuable information about the band parameters and in uncovering the hills and dales of the Fermi surfaces. This is particularly true in the temperature range that cannot be explored by the more powerful quantum effects, i.e. above the liquid helium temperature range.

Most of the properties that distinguish the group V semimetals from the less exotic isotropic metals or semiconductors are due to their particular crystallographic

* Paper presented at the AIP Solid State Physics Meeting, Wagga Wagga, N.S.W., 7–9 February 1979.

structure. This structure, which is rhombohedral, may be considered as a slightly distorted cubic one, and this distortion is responsible for the overlap between the conduction and valence bands. The overlap is, however, much smaller in semimetals than that which occurs in some metals.

The Fermi surface of the group V semimetals is known with great accuracy at low temperatures. In bismuth and antimony, it was found to consist of sets of ellipsoids, whose sizes, locations and tilt angles in momentum space have been correctly determined. In arsenic, the Fermi surface has a whimsical shape reminiscent of a drawing from some schizophrenic artist. Fortunately, for the purpose of analysis of transport properties it can be approximated by ellipsoids. Non-parabolicity has been detected for some of the bands in bismuth and this has been found to affect the transport properties. What we do not know yet is how these Fermi surfaces are modified when the temperature increases above the liquid helium range. The problem is not critical for arsenic and antimony below room temperature, since the situation is comparable with that of metals, i.e. a temperature-independent Fermi surface and carrier population may be assumed. For bismuth, however, this assumption is not valid and we require the transport coefficients to obtain some information about the temperature dependence of the Fermi energies. Unfortunately, for this purpose, we need to make some reasonable assumptions about the scattering processes, and this is not easy.

In the study of transport properties, one is concerned with particles whose movement, initially isotropic, is directed in a preferred orientation under the action of external forces. The particles concerned here are electrons and holes, which are best described by their Fermi surfaces, and phonons, whose dispersion relations may be determined experimentally. Collisions tend to bring the particle system back into equilibrium and the relaxation time is the essential parameter describing the process. In the temperature range in which we are interested here, i.e. below room temperature, the charge carriers are scattered by phonons, impurities and boundaries. The phonons are mainly scattered by other phonons, impurities, boundaries and eventually by charge carriers. One particular case, which needs to be considered for group V semimetals, is where there is an anisotropic transfer of momentum between the phonon and charge carrier systems leading to the so-called phonon-drag effects.

We shall be mainly concerned here with three essential transport properties: the electrical resistivity ρ, the thermal conductivity κ, and the thermopower α. Although the effect of magnetic field will be briefly discussed, we shall mainly concentrate on the zero-field coefficients, since they are easier to visualize. From symmetry arguments, it may be shown that, for the three zero-field transport properties, the tensors have only two components, one along the trigonal axis that we shall denote $\rho_{\parallel}$, $\kappa_{\parallel}$ and $\alpha_{\parallel}$, and one in the plane perpendicular to this axis (the trigonal plane) that we shall denote $\rho_{\perp}$, $\kappa_{\perp}$ and $\alpha_{\perp}$. For the charge carrier spectrum, two distinct temperature regions will be considered: one which may be described as fully degenerate, that we shall call the 'degenerate' region, and one for which exact Fermi–Dirac statistics should be used, that we shall call the 'partially degenerate' region. Practically, for arsenic and antimony we are in the degenerate region up to room temperature, while for bismuth this will only hold below ~ 60 K. Above this temperature, we are in the partially degenerate region for bismuth and the situation will be far more complicated to analyse.

The present survey is mainly addressed to solid state physicists who are not familiar with semimetals. This is why, when possible, we will be comparing the properties discussed with those of the more familiar semiconductors or metals. A study of the transport properties of group V semimetals is not only interesting *per se* but also introduces some particular situations that do not occur with other solids. As an example, it is the only way to study a partially degenerate system, or a compensated material, without having dominant impurity scattering. Also, by comparing the properties of the three group V semimetals, one may observe how a given property varies in a fully degenerate system when the Fermi energies vary by orders of magnitude. In the particular field of thermal conductivity, one has the opportunity to examine different low temperature mechanisms for heat conduction in the same material.

Throughout the following text, we shall lean heavily on the physics of the different effects under study, rather than on their formal representation. We shall thus keep the mathematics at the lowest possible level that is compatible with the complexity of the situations involved. Also in what follows, bismuth will be given particular attention for two reasons: The more obvious one is that it is the material which has been the most extensively studied because it is very easy to grow while, at the other end of the scale, arsenic is very difficult to obtain in the form of single crystals and is delicate to handle. The other reason is that bismuth is the most typical semimetal, or rather the most semimetallic of the group, since it has by far the lowest carrier densities. The other two semimetals, arsenic and antimony, behave almost like typical metals below room temperature, the range for which most of the experimental data are available.

2. Band Structure

The group V semimetals are mainly characterized by their rhombohedral crystal structure, which is responsible for the small overlap between the valence and conduction bands (Fig. 1). This leads to the presence of a small equal number of electrons and holes at all temperatures (Fig. 2).

The band structure at 0 K and the electronic parameters of the group V semimetals are quite well known now and have been reviewed extensively (e.g. Boyle and Smith 1963; Dresselhaus 1971; Edelman 1976). We wish to show here how the anisotropy due to the rhombohedral crystal structure, and the band structure resulting from the distortion from cubic symmetry, distinguish the group V semimetals from the more commonly known isotropic insulators or metallic conductors.

(a) Comparison with other crystalline solids

The difference between an insulator and a semiconductor is of a quantitative nature: it is only the magnitude of the energy gap which distinguishes between them. A particular case of semiconductors is that of the narrow-gap materials;* their gap is usually less than a few tenths of an electron-volt while in a typical semiconductor it is nearer to 1 eV. All three types of materials are insulators at 0 K. On the other hand, semimetals, as well as metals, are good conductors at 0 K. It is the degree of overlap between the valence and conduction bands that differentiates between them

* It would be interesting to compare the properties discussed here with those of the narrow-gap semiconductors, since they have some common features with the group V semimetals (Zawadzki 1974).

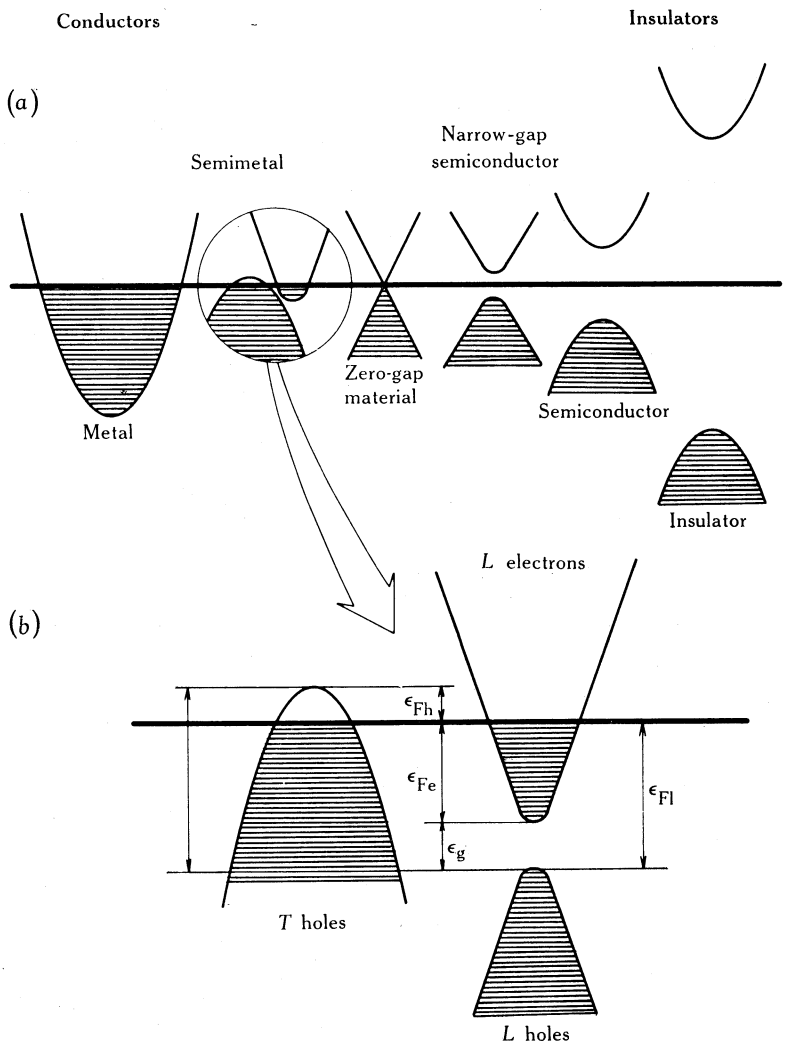

Fig. 1. Comparison (*a*) of the band structure of semimetals with that of other crystalline solids at low temperatures, namely metals with a high electronic population and insulators with a large energy gap. The band structure of bismuth at 0 K is represented in (*b*); here ε_{Fe}, ε_{Fh} and ε_{Fl} are the Fermi energies of electrons, heavy holes and light holes respectively, while ε_g is the direct energy gap.

or, in other words, the density of free carriers at 0 K. While the Fermi energies are of the order of eV in metals, they are usually below a few tenths of an eV in semimetals (Table 1). The Fermi energies of electrons or holes are specified with respect to the energy extrema in the corresponding electron and hole carrier pockets, as indicated in Fig. 1. In this figure, the band structures of various kinds of crystalline solids are also schematically represented. It may be seen how the band structure varies from the typical metal, i.e. a partially filled band at 0 K which may be due to a large overlap, to an insulator with a large energy gap. The difference in the electronic

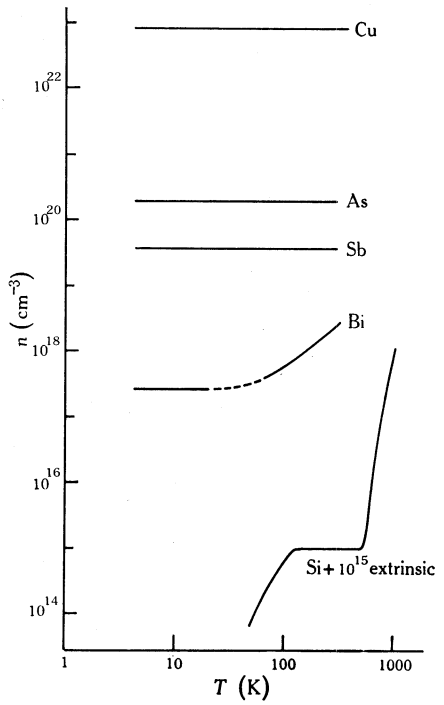

Fig. 2. Comparison of the temperature variation of the carrier density n of group V semimetals with that of a metal (copper) and a typical semiconductor (silicon, with $\sim 10^{15}$ cm^{-3} impurity concentration). Note that below room temperature, arsenic (Jeavons and Saunders 1969) and antimony (Oktü and Saunders 1967*a*) have an almost temperature-independent carrier density like metals. In bismuth (Michenaud and Issi 1972) this is the case at very low temperatures but at higher temperatures the carrier density increases with temperature, as is the case for silicon above and below the exhaustion region.

Table 1. Band parameters for carriers in semimetals at liquid helium temperatures

Of the parameters listed, ϕ_e and ϕ_h are the tilt angles of the electron and hole ellipsoids respectively, N_v is the number of valleys in the Fermi surface, and the other symbols are explained in the text

Semimetal carriers	$m_{1'}$ (m_0 units)	$m_{2'}$ (m_0 units)	$m_{3'}$ (m_0 units)	$\phi_e(2 \to 2')$ (deg)	$\phi_h(3 \to 2')$ (deg)	ε_F (meV)	$n = p$[A] (cm^{-3})	N_v
Bismuth								
electrons	0·00119	0·266	0·00228	6·0±0·2	—	27·2	2·7(17)	3
holes	0·064	0·064	0·69	—	0	10·8	2·7(17)	1
Antimony								
electrons	0·093	1·14	0·088	−4	—	93·1	3·74(19)	3
holes	0·068	0·92	0·050	—	53	84·4	3·74(19)	6
Arsenic								
electrons	0·135	1·52	0·127	−4	—	202	2(20)	3
α holes	0·106	1·56	0·089	—	37·5	154	2(20)	6
γ holes	0·046	0·016	−1·82	—	−9·6	21	~3(18)	6

[A] Values in parentheses are the power of the 10 multiplier, i.e. $2{\cdot}7(17) \equiv 2{\cdot}7 \times 10^{17}$.

structure between a metal and a semimetal will have important consequences for the transport properties. Firstly, in comparison with metals, a smaller density of carriers will lead to a smaller conductivity (see Section 3*a* below) and eventually to relatively important densities of thermally excited carriers at higher temperatures, when compared with the density of carriers initially present at 0 K. This is particularly true for the case of bismuth, which is 'metallic' at low temperatures and has an increasing carrier population at higher temperatures, as is the case for semiconductors.

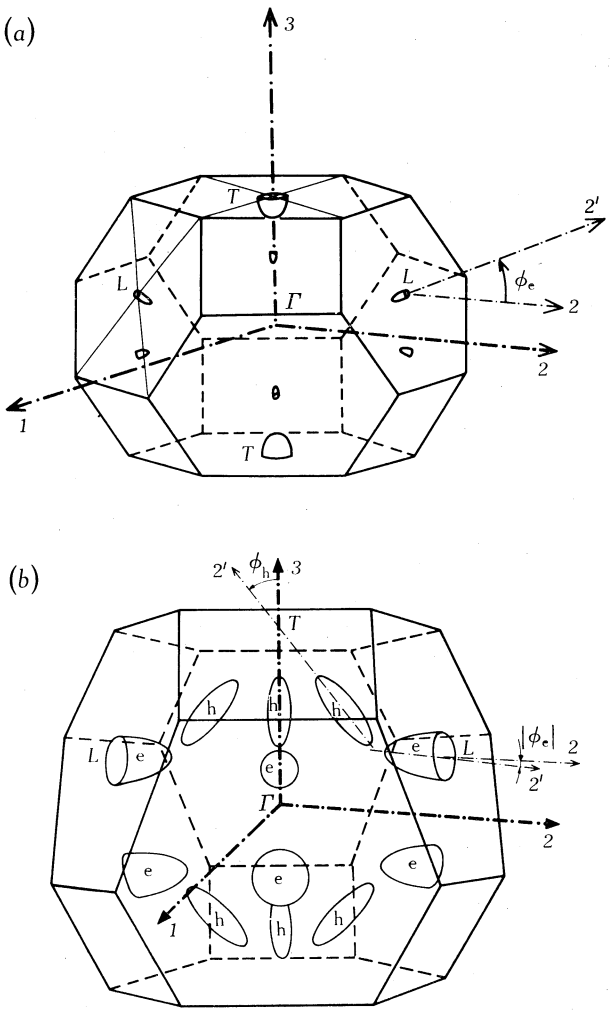

Fig. 3. Fermi surfaces of the group V semimetals:
(*a*) Location of the Fermi surfaces of bismuth in the Brillouin zone: the holes at *T* points and the electrons at *L* points. Note that the volume of each ellipsoid is approximately 10^{-5} that of the Brillouin zone.
(*b*) Location of the Fermi surfaces of arsenic and antimony in the Brillouin zone; e and h are the electron and hole pockets respectively.
(*c*) Hole Fermi surface of arsenic centred at the *T* point of the Brillouin zone.
In (*a*) and (*b*), ϕ_e and ϕ_h are the tilt angles of the electron and hole ellipsoids.

A smaller carrier density will also facilitate the observation of quantum oscillations at low temperatures and allow the transport properties to be drastically altered by doping. The second consequence is that a very small direct band gap, when present, will be responsible for non-parabolicity of interacting bands, as is the case for some narrow-gap semiconductors. Thirdly, a band structure that is very sensitive to

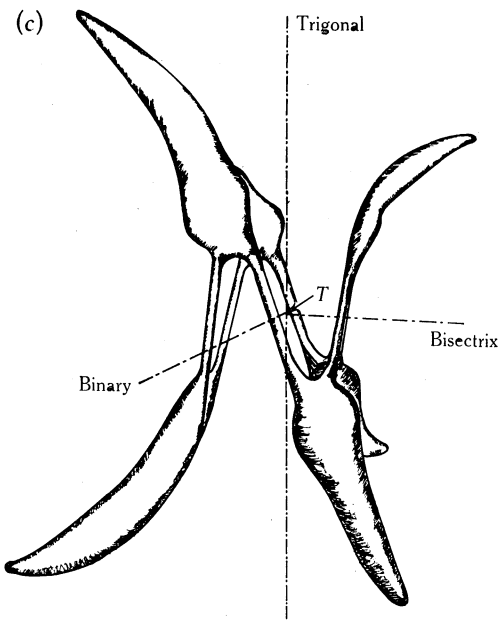

Fig. 3c [see caption on facing page]

temperature (Vecchi and Dresselhaus 1974), as is the case for bismuth, can be expected to have important effects on the transport properties. In other solids, it is usually a good approximation to assume that the band structure is temperature independent. These considerations will now be put into a quantitative form.

(*b*) *Dispersion relation*

While the valence band of bismuth together with both the valence and conduction bands of antimony and arsenic have been up to now successfully described by a simple parabolic model, there have been many models proposed for the dispersion relation of the conduction band of bismuth. This has resulted from the experimental observation of an effective mass variation with energy in the conduction band (Keyes *et al.* 1956), which has been attributed to the presence of a very small energy gap ε_g between the conduction band and a lower lying valence band at the L point of the Brillouin zone (Fig. 3*a*), which leads to a non-parabolic dispersion relation. The various dispersion relations proposed for these bands have been recently reviewed by Mc Clure and Choi (1977). We shall only retain here those relations which are the most commonly used, since they have a direct impact on the transport properties in which we are interested.

(i) *Parabolic Model*

Except for the conduction band of bismuth, the dispersion relations for the conduction and valence bands of the three group V semimetals are parabolic. This

means that the ellipsoidal isoenergetic surfaces in k space are described by the well-known relation

$$\varepsilon(k) = (\hbar^2/2m_0)\,\boldsymbol{k}\,\mathbf{m}^{-1}\,\boldsymbol{k}, \tag{1}$$

where ε is the energy, m_0 the free electron mass and $\mathbf{m}^{-1}$ a symmetric dimensionless reciprocal effective mass tensor. Since the principal axes of the isoenergetic surfaces are usually tilted with respect to the crystallographic axes, one should specify the frame of reference for $\mathbf{m}^{-1}$, that is, either the crystallographic axes or the principal axes of the energy surfaces. In the latter case one may write

$$\mathbf{m}^{-1} = \begin{bmatrix} m_{1'} & 0 & 0 \\ 0 & m_{2'} & 0 \\ 0 & 0 & m_{3'} \end{bmatrix}^{-1}, \tag{2}$$

where $m_{1'}$, $m_{2'}$ and $m_{3'}$ are the components of the effective mass tensor expressed in units of m_0. In Table 1, the effective masses of the group V semimetals are given at 0 K. A representation of the Fermi surfaces of the three group V semimetals is given in Fig. 3.

(ii) *Non-parabolic Models*

The infrared cyclotron resonance measurements of Keyes *et al.* (1956) suggested that the effective mass m^* cannot be taken as a constant for the band, but instead is a function of the energy ε. Thus, if m is an effective mass tensor element at the band extremum, then

$$m^*(\varepsilon) = m(1 + 2\varepsilon/\varepsilon_g). \tag{3}$$

This expression was first derived by Kane (1957) for indium antimonide and later applied to bismuth by Lax and Mavroides (1960) using a $\boldsymbol{k}.\boldsymbol{p}$ perturbation technique. The dispersion relation in this case takes the more general form

$$\gamma(\varepsilon) = (\hbar^2/2m_0)\,\boldsymbol{k}\,\mathbf{m}^{-1}\,\boldsymbol{k}, \tag{4}$$

where $\mathbf{m}^{-1}$ is now the reciprocal effective mass tensor at the band extremum. Equation (4) is similar to (1) except that $\gamma(\varepsilon)$ is now a function of the energy:

$$\gamma(\varepsilon) = \varepsilon(1 + \varepsilon/\varepsilon_g). \tag{5}$$

This relation describes what is usually called the 'Lax model'. In this model the isoenergetic surfaces are still ellipsoids in k space and they may be represented by combining equations (4) and (5) to give

$$\varepsilon(k) = \pm\tfrac{1}{2}(\varepsilon_g^2 + 2\varepsilon_g\hbar^2 m_0^{-1}\,\boldsymbol{k}\,\mathbf{m}^{-1}\,\boldsymbol{k})^{\frac{1}{2}} - \tfrac{1}{2}\varepsilon_g. \tag{6}$$

The Lax model is thus also called the ellipsoidal non-parabolic (ENP) model. Cohen (1961) developed a non-ellipsoidal non-parabolic (NENP) model which takes into account the experimental fact that the electron mass component $m_{2'}$ is much larger than the other two components $m_{1'}$ and $m_{3'}$. Since the transport properties are not very sensitive to the differences between the ENP and NENP models, we shall hereafter use the first model (ENP) which has the advantage of being relatively easier to handle in some instances.

(*c*) *Pseudoparabolic model*

The pseudoparabolic model uses the Lax dispersion relation to consider the scattering of electrons in bismuth. It was recently derived by Heremans and Hansen (1979) and it accounts for the effect of non-parabolicity in both the density of states and the electron–phonon matrix element.

In the previous section the non-parabolicity was taken into account in deriving the dispersion relation of the conduction band of bismuth. However, the existence of the *L*-point direct energy gap will also affect the wavefunctions of the carriers. These will become a linear combination of functions describing the interacting bands. Since the coefficients of this combination are energy dependent, so will be the electron–phonon matrix element, and this must be taken into account in the analysis of the transport effects. Ravich *et al.* (1971) and Zawadzki and Szymanska (1971) first introduced this concept and derived the relevant expressions for the case of narrow-gap semiconductors, namely the lead chalcogenides and indium antimonide respectively. This model, when applied to bismuth in the degenerate region, was successful in reconciling, after two decades of controversy, the theory of the diffusion thermopower with the experimental results around 60 K (see Section 5*a*).

(*d*) *Fermi energies*

One important thing to take into account in the study of semimetals is the relative magnitude of $k_B T$ with respect to ε_{Fe} and ε_{Fh}, the Fermi energies for electrons and holes respectively. This will determine the degree of degeneracy of the carrier statistics, and in this respect arsenic and antimony will be quite different from bismuth. For arsenic and antimony one may reasonably assume that ε_{Fe} and ε_{Fh} are much greater than $k_B T$ below room temperature and thus use fully degenerate statistics to describe the situation. This will also apply to bismuth below about 60 K, and the situation will not be much different from that encountered in typical metals; i.e. the carrier density will remain almost temperature independent in this range (Fig. 2). This will simplify the interpretation of the temperature dependence of the transport properties. However, for bismuth above 60 K we can no longer assume $\varepsilon_{Fe}, \varepsilon_{Fh} \gg k_B T$, and exact Fermi–Dirac statistics must be used to describe the carrier system. Also the carrier density is temperature sensitive and increases by about an order of magnitude from 4·2 to 300 K (Fig. 2), a situation qualitatively similar to that encountered in semiconductors. The origin of the increase of the carrier density with temperature in bismuth is not yet fully understood.

The density of carriers (n or p) may be determined from the measurement of the galvanomagnetic effects (see Section 6*b*). From this result the Fermi energies may be evaluated at a given temperature provided the effective masses are known. For parabolic bands, the density of free carriers per valley is given by

$$n = \frac{8\pi(2m_0)^{3/2}}{3h^3}(\det \mathbf{m})^{1/2} \int_0^\infty \varepsilon^{3/2}(-\partial f_0/\partial\varepsilon)\, \mathrm{d}\varepsilon, \tag{7}$$

where f_0 is the equilibrium Fermi–Dirac distribution function

$$f_0 = \left(1 + \exp\{(\varepsilon - \varepsilon_F)/k_B T\}\right)^{-1}. \tag{8}$$

For $\varepsilon_F \gg k_B T$, the expression (7) reduces to (Heremans and Hansen 1979)

$$n = \{8\pi(2m_0)^{3/2}/3h^3\}(\det \mathbf{m})^{1/2}\varepsilon_F^{3/2}. \tag{9}$$

This relates to the Fermi energy the electron and hole density in arsenic and antimony below room temperature, and the hole density in bismuth below 60 K. If, however, we have $\varepsilon_F \sim k_B T$, the full expression (7) has to be used, and this will relate to the Fermi energies the hole density in bismuth above 60 K. It will also apply to electrons and holes in antimony above room temperature.

For the electron band in bismuth, we must take into account the non-parabolicity. In this case, the expression for the carrier density per valley reads

$$n = \{8\pi(2m_0)^{3/2}/3h^3\}(\det \mathbf{m})^{1/2}\int_0^\infty \gamma^{3/2}(\varepsilon)(-\partial f_0/\partial\varepsilon)\,\mathrm{d}\varepsilon \tag{10}$$

and, for $\varepsilon_F \gg k_B T$,

$$n = \{8\pi(2m_0)^{3/2}/3h^3\}(\det \mathbf{m})^{1/2}\gamma^{3/2}(\varepsilon_F). \tag{11}$$

This is identical with equation (9) except that $\varepsilon_F^{3/2}$ is now replaced by $\gamma^{3/2}(\varepsilon_F)$.

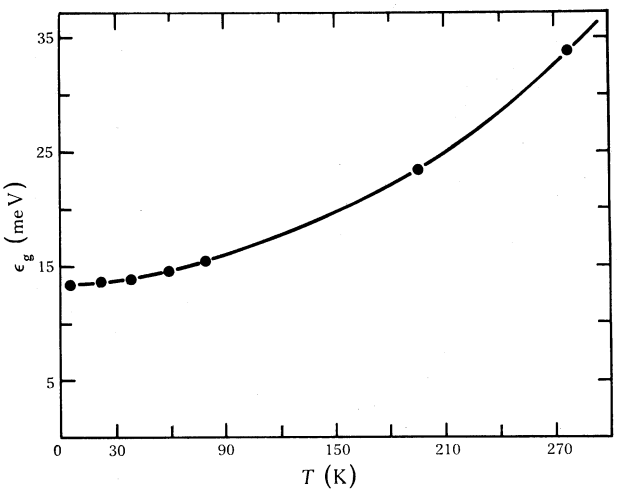

Fig. 4. Temperature variation of the *L*-point direct energy gap ε_g of bismuth (from Vecchi and Dresselhaus 1974). The gap has a value of 13·6 meV at low temperatures and reaches 37 meV around 300 K.

(e) *Temperature variation of band parameters*

The effective masses and Fermi energies may be determined accurately in the liquid helium range by using the sophisticated armoury of quantum oscillatory effects (see e.g. Dresselhaus 1971). Once this is achieved, one may reasonably assume that these parameters will remain unchanged up to room temperature in antimony and arsenic. Until 1974, this was usually accepted for bismuth too. However, by extending their magnetooptical measurements up to room temperature, Vecchi and Dresselhaus (1974) were able to observe a drastic variation of the band parameters with increasing temperature. In Fig. 4, the variation of ε_g with temperature is repre-

sented. It may be seen that, at room temperature, ε_g is about three times larger than at 4·2 K. The temperature variation of the gap may be expressed as

$$\varepsilon_g = \varepsilon_{g0} + 2{\cdot}1 \times 10^{-3} T + 2{\cdot}5 \times 10^{-4} T^2 \quad \text{meV}, \tag{12}$$

where ε_{g0} is the value of ε_g at 0 K ($\varepsilon_{g0} = 13{\cdot}6$ meV). Since this is the smallest gap whose temperature dependence has ever been measured in solids, one general conclusion may be drawn at this stage. If one refers to measurements performed on a large number of semiconductors (Bube 1960), the absolute variation of the energy gap per unit temperature (Table 2) is generally of the same order for most of the crystalline solids. However, the relative increase or decrease with respect to the 0 K value ε_{g0} may vary drastically from one solid to another. While in typical semiconductors, such as germanium or silicon, the relative effect is usually very small and may be neglected in the analysis of transport properties, in narrow-gap materials, and especially in bismuth, the relative effect is dramatic. Note also that a general trend in semiconductors is that small effective masses are associated with small energy gaps and bismuth is no exception to this general rule (Table 1).

Table 2. Absolute and relative energy gap variation per unit temperature in some typical solids

Material	Absolute ε_g variation β (10^{-4} eV K^{-1})	ε_g at 0 K ε_{g0} (eV)	Relative ε_g variation β/ε_{g0} (10^{-4} K^{-1})
Si	−4	1·1	−3·6
Ge	−4·5	0·7	−6·4
PbTe	+4	0·31	+13
InSb	−2·7	0·18	−15
Bi	∼+1[A]	0·013	+77

[A] This is only a rough estimate since the variation of ε_g with T in bismuth is not linear (equation 12).

In bismuth, the effective masses at the band extrema are also very sensitive to temperature (Vecchi and Dresselhaus 1974). However, since the bisectrix mass m_2 is much larger than the two other masses (m_1 and m_3), it is less accessible experimentally. So, in order to deduce the Fermi energies from equation (10) in the higher temperature range, one must speculate about the temperature variation of m_2. This considerably complicates the analysis of the transport properties of bismuth above 60 K (Heremans and Hansen 1979). It is worth noting that, while the masses at the bottom of the band increase with increasing temperature, the effect of the gap variation ε_g tends to decrease the non-parabolicity of the band (equation 3) with increasing temperature. These combined effects should be considered when evaluating the variation with temperature of the effective mass at a given energy.

At this stage, one may rightly question the relevance of using the effective mass concept when describing the properties of electrons in bismuth. In fact, when it was first introduced for semiconductors, this concept had the obvious advantage of simplifying our understanding of the dynamic behaviour of the charge carriers by taking into account, using a constant parameter, all the lattice forces acting on them. When, as is the case now, we find that, in order to be consistent with new experimental observations, the effective masses must vary with energy and with temperature,

we should consider revising the position and treat the transport properties in a more formal way.

Another consequence of the smallness of the gap ε_g is that, when $k_B T$ becomes comparable with ε_g, direct excitation is expected to occur from the light hole band to the electron band, thus allowing additional carriers to contribute to transport phenomena. This is a situation similar to that occurring in narrow-gap semiconductors and one could apply the same formulae to estimate the density of carriers so excited, provided allowance was made for the temperature variation of the energy gap. Up to room temperature, the density of these carriers should not exceed about 10% of the total population.* The additional electrons generated will thus not affect to a great extent the overall qualitative behaviour of the conduction band. With regard to holes, since the light holes generated at the L point have different characteristics from those dominating the scene, namely the T holes, they may affect drastically some of the transport properties. A useful comparison could be made with the situation prevailing in p-type germanium, except that for this case the extrema of the two bands, namely light and heavy holes, coincide in k space.

3. Electrical Resistivity

The enormous magnetoresistance and Hall effect of bismuth facilitated to a great extent the early observations of these effects. The effects are indeed much more pronounced in this material than in typical metals or even in the two other group V semimetals, and only rather simple experimental set-ups were needed for the measurements. These dramatic effects stem directly from the very high carrier mobilities, especially at low temperatures. Increases in resistivity in a magnetic field, exceeding by 10^6 times their zero-field value, were reported in the liquid helium range (Alers and Webber 1953). Less spectacular, and more tedious for the experimentalist, was the systematic investigation of the low-field galvanomagnetic effects, which relied on the measurement of minute effects. However, these studies proved very rewarding since the results were found to be a useful basis for determination of the temperature variation of the band parameters (Abeles and Meiboom 1956; Oktü and Saunders 1967*a*; Jeavons and Saunders 1969; Michenaud and Issi 1972).

In isotropic monovalent metals or extrinsic semiconductors, where only one type of carrier is present, the carrier density n and mobility μ may be readily determined experimentally by measuring the Hall coefficient

$$R_H = \pm(en)^{-1}, \tag{13}$$

from which n is directly available, and the electrical resistivity

$$\rho = (en\mu)^{-1}, \tag{14}$$

from which the mobility is deduced once n is known. In group V semimetals, although the same types of relations are still applicable, the strong anisotropy, as well as the simultaneous presence of at least two types of carriers, lead to complicated relations

* Note that the temperature variations of the carrier densities in bismuth represented in Fig. 2, which are the values generally accepted, were obtained by assuming only two-band conduction in this material (Michenaud and Issi 1972).

between the measured coefficients and the electronic parameters. Also, an increase in the number of necessary experiments will be required.

The galvanomagnetic effects will be discussed in Section 6*a* below. However, we shall start by reviewing in more detail the zero-field resistivity, since it allows a better physical insight into the scattering mechanisms in the group V semimetals.

(*a*) *Anisotropy and temperature variation*

The results of measurements of the temperature variation of the resistivities of the three group V semimetals are rather puzzling and still only partially explained.

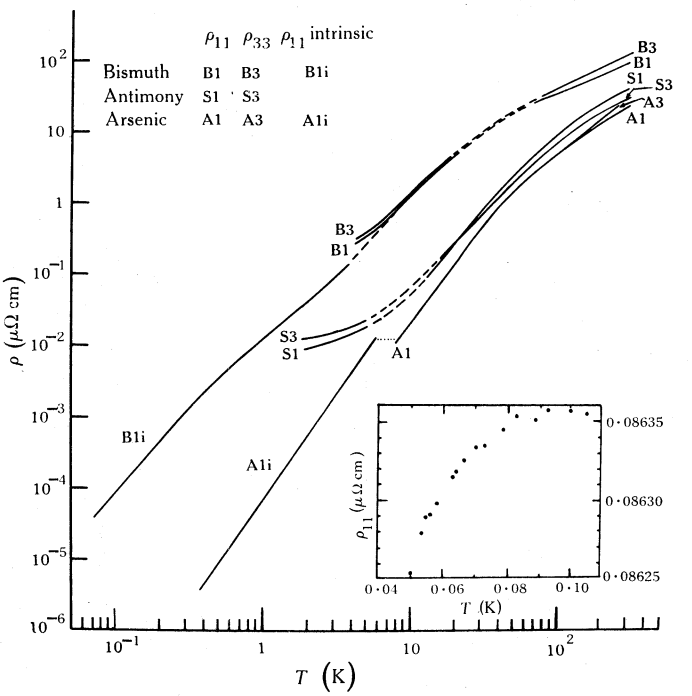

Fig. 5. Temperature variation of the electrical resistivity ρ of the three group V semimetals. Note that the anisotropy of the ideal resistivity is not very large for group V semimetals around room temperature, and that it almost disappears at low temperatures. The insert shows the start of the decrease in resistivity of a binary arsenic sample at very low temperatures (from Uher 1978*a*). The indices 11 and 33 denote the binary and trigonal directions respectively.

Because of the high anisotropy of the properties of the semimetals, which is reflected in the mobilities, one should expect the two resistivity components $\rho_{\parallel}$ and $\rho_{\perp}$ to be quite different. However, this is not the case. At high temperatures the two components are not so different and, what is more striking, they become almost equal at lower temperatures (Fig. 5). In fact, when equation (14) is extended to two-band conduction, one gets

$$\rho = \{en(\mu_e + \mu_h)\}^{-1}, \tag{15}$$

where the subscripts e and h refer to electrons and holes respectively.

From the data available in the literature and with the assumed validity of Matthiessen's rule

$$\rho_i = \rho - \rho_r, \tag{16}$$

where ρ is the total measured resistivity and ρ_r the residual resistivity, the temperature variation of the ideal resistivity ρ_i is plotted in Fig. 5. For the cases of arsenic and antimony, since the carrier density is assumed to be almost temperature independent up to 300 K, one would expect the temperature variation of the conductivity to reflect entirely that of the mobilities. Pure acoustic intravalley electron–phonon scattering predicts a linear variation with T at high temperatures and a T^5 dependence at very low temperatures. For arsenic, three sets of measurements are reported in the literature covering the temperature range from 0·05 to 305 K. Values of $\rho_{\parallel}$ and $\rho_{\perp}$ were reported by Jeavons and Saunders (1969) from 77 to 305 K, while $\rho_{\perp}$ was measured by Heremans *et al.* (1977) from 2·3 to 296 K and by Uher (1978*a*) from 0·05 to 6 K. We may see from Fig. 5 that there is no sign of a linear temperature variation at high temperatures. At low temperatures, instead of a T^5 dependence, a T^3 variation is observed below 30 K with a different coefficient according to the temperature range considered.

For antimony, $\rho_{\parallel}$ and $\rho_{\perp}$ were reported by Oktü and Saunders (1967*a*) from 77 to 273 K, by Tanaka *et al.* (1968) from 77 to 300 K and by Bressler and Red'ko (1971) from 1·9 to 300 K. The power dependence of ρ on T is continuously variable from slightly above 1 at room temperature to 2·5 around 77 K. From the only low temperature data available for $\rho_{\parallel}$ and $\rho_{\perp}$ (Bressler and Red'ko 1971), it is not possible to separate ρ_i from ρ_r, since at 1·9 K the total resistivities are still temperature dependent. However, measurements reported by Bansal and Duggal (1973) on $\rho_{\perp}$ showed that the ideal resistivity of this component varies as T^3 from 4·2 to 20 K, confirming the early results of White and Woods (1958), who reported a $T^{2\cdot75}$ variation for polycrystalline material. In this case the behaviour is similar to that of arsenic.

For bismuth, the situation is even more surprising. We note that from 77 to 300 K the resistivities $\rho_{\parallel}$ and $\rho_{\perp}$ vary almost linearly with temperature (Gallo *et al.* 1963; Michenaud and Issi 1972). This behaviour, which was interpreted by earlier workers as a sign of metallic conduction, is totally misleading. While in metals, and probably in the two other semimetals, only the relaxation time τ varies with temperature, in bismuth, as we have already seen (Section 2) not only the carrier densities vary dramatically with temperature but also their effective masses. Thus the temperature variation of the mobility will depend on that of the two parameters m and τ:

$$\mu = e\tau/m. \tag{17}$$

In this semimetal, where we certainly would not have expected a linear variation of the resistivity, we find it. At lower temperatures, there is the T^2 variation first reported by White and Woods (1958) for polycrystalline material and further confirmed by many investigators on single crystal samples (Bhagat and Manchon 1967; Friedman 1967; Fenton *et al.* 1969; Hartman 1969; Chopra *et al.* 1971; Kopylov and Mezhov-Deglin 1974; Kukkonen and Sohn 1977; Uher and Pratt 1977). But

this variation still remains a matter for conjecture (Anagnostopoulos and Aubrey 1976; Kukkonen and Maldague 1976).

Apart from the temperature dependence, there are other observations for the electrical resistivities which need to be considered. The relatively small number of free carriers in group V semimetals leads one to expect correspondingly small electrical conductivities. In bismuth, for example, n at room temperature is more than four orders of magnitude smaller than in typical metals (see Fig. 2), but the conductivity is only two orders of magnitude smaller. This, we know, is related to the very high mobilities of the carriers in the group V semimetals as compared with that of typical metals. When we look at the expression (17) for the mobility and at Table 1 we note that the very small effective masses will obviously lead to high mobilities in some directions. However, this is not the only reason. The relaxation times of the charge carriers will also be relatively large in semimetals compared with those of metals, for a reason which is not fundamentally different from the one invoked for semiconductors. In fact, it was realized early by Sondheimer (1952) that intravalley electron–phonon interactions in semimetals should be different from those in ordinary metals. Energy and momentum conservation require that electrons interact with phonons of wave number $q \leqslant 2k_F$, where k_F is the Fermi wave number. Since in momentum space the Debye sphere is much larger than the Fermi surface at high temperatures ($T > \theta_D$, where θ_D is the Debye temperature), the electrons will interact with low energy phonons, as opposed to the thermal phonons of energy $k_B\theta_D$ which dominate the scene above θ_D. In fact, the important parameter here is not the Debye sphere, or the corresponding temperature θ_D, but instead an effective temperature for carrier–phonon interaction θ^*, which is given by

$$\theta^* = 2k_F v_s \hbar/k_B, \tag{18}$$

where v_s is the velocity of sound.

Now, because the Fermi surfaces are highly anisotropic in the degenerate region so will be θ^*, and the interacting phonons will be entirely confined in an ellipsoid in momentum space, with semi-axes of twice the length of the semi-axes of the Fermi ellipsoid of the charge carriers with which they interact. Since below θ_D the energy of the dominating phonons is proportional to $k_B T$, only at very low temperatures will the dominant phonons have wave vectors of the order of the Fermi wave vectors. These considerations will also apply when we discuss the phonon-drag effects (Section 5*b*).

(*b*) *Effect of non-parabolicity*

It is worth asking now whether the non-parabolicity will affect the scattering mechanism of electrons in bismuth. The answer is given by Heremans and Hansen (1979) in the framework of their pseudoparabolic model. In the fully degenerate region, in the case of pure acoustic phonon intravalley scattering, the energy dependence of the relaxation time τ for a parabolic band is given by

$$\tau = \tau_0(\varepsilon/k_B T)^{-\frac{1}{2}}. \tag{19}$$

In the pseudoparabolic model, where the effect of non-parabolicity is taken into

account in both the density of states and the electron–phonon matrix element (Heremans and Hansen 1979),

$$\tau = \tau_0(\gamma/k_B T)^{-\frac{1}{2}}\gamma', \tag{20}$$

where

$$\gamma' = \partial\gamma/\partial\varepsilon = 1 + 2\varepsilon/\varepsilon_g. \tag{21}$$

Heremans and Hansen have shown that both the parabolic and pseudoparabolic models lead to the same expression for the mobility when it is expressed as a function of the electron wave number k:

$$\mu = e\tau_0(2k_B T/m)^{\frac{1}{2}}(\hbar k)^{-1}, \tag{22}$$

and so the non-parabolicity will not affect the dependence of the mobilities on k.

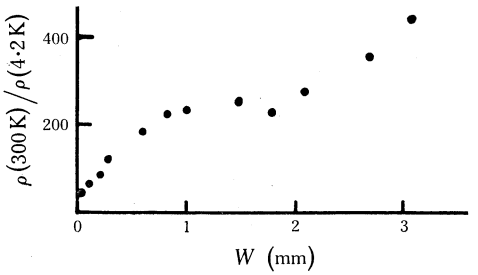

Fig. 6. Typical size effect in the electrical conductivity of binary bismuth samples at 4·2 K (from Garcia and Kao 1968). The electrical conductivity decreases first with thickness W, levels off, and then decreases again with further decrease in thickness.

(c) *Size effects*

In bismuth, one other puzzling observation, which is now well established experimentally, is the variation of the electrical conductivity σ with sample size in the liquid helium range (Friedman and Koenig 1960; Friedman 1967; Garcia and Kao 1968; Aubrey and Creasey 1969; Issi and Mangez 1972; Kopylov and Mezhov-Deglin 1974). In ordinary metals, and even in antimony (Aleksandrov *et al.* 1972), when the mean free path is of the order of a dimension of the sample, there is a steady decrease of conductivity with this dimension at a given temperature. This is due to the scattering of electrons at the boundaries of the sample. In bismuth, however, after a first decrease with thickness, the conductivity levels off, followed by a further decrease (Fig. 6). It is interesting to note that, because of size effects, in the liquid helium range, no measurements have ever been reported on a bismuth bulk specimen. These size effects are even more dramatic in the thermopower, as will be seen in Section 5. Many explanations have been proposed invoking the complexity of the Fermi surface, specular and diffuse contributions, phonon-drag effects or intervalley and surface effects. The definite answer is still not obvious and probably there is more than one simple mechanism that is responsible for this peculiar behaviour. We shall discuss one of these aspects while considering phonon-drag effects (Section 5*b*).

(d) *Superconductivity at ultralow temperatures*

One of the most exciting possibilities in the field of ultralow temperature transport in semimetals is the possible occurrence of superconductivity in the pure crystalline

material. Tin-doped bismuth samples were found by Uher and Opsal (1978) to be superconducting with a vanishing resistance around 0·03 K (Fig. 7). The transition temperature increased with the concentration of the dopant. A reasonable extrapolation of the transition temperature curve versus tin content suggests that pure bismuth might also be superconducting at around 10^{-2} K. In the same way, the resistivity of a tellurium-doped sample was found to start to drop rapidly. In both cases the critical fields were very low. Uher (1978*a*) has reported also that the resistivity of a binary arsenic sample started to drop rapidly at around 0·05 K, the lowest temperature attained (Fig. 5). This behaviour suggests that there might be the beginning of a superconducting transition and, if confirmed by extending the measurement to lower temperatures, it would be the first experimental observation of superconductivity in a pure crystalline semimetal, if we exclude high pressure measurements.

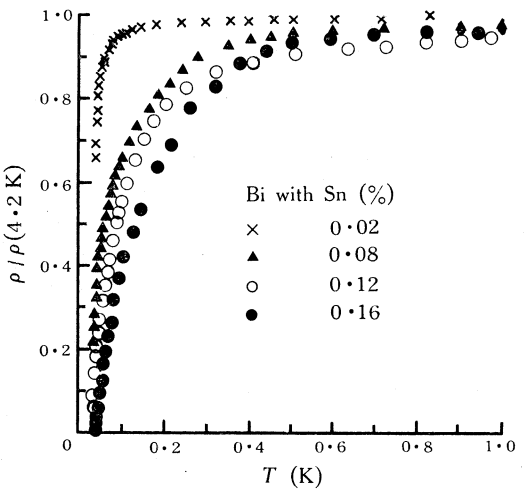

Fig. 7. Superconducting results in tin-doped polycrystalline samples of bismuth with the indicated different tin concentrations (from Uher and Opsal 1978).

(*e*) *Some practical points*

One particular problem, to which the experimentalist should be attentive, is the fact that it is difficult to realize isothermal conditions when measuring the DC electrical resistivity of semimetals, and especially of bismuth in certain temperature ranges. From a macroscopic viewpoint, when an electric current I flows in a conductor of resistance R, the resulting e.m.f. V is, generally speaking, the sum of two terms:

$$V = RI + \alpha \Delta T. \tag{23}$$

The first term, RI, is the ohmic term, in which we are interested, and the second, $\alpha \Delta T$, is a thermoelectric voltage caused by the Peltier effect, where α is the thermopower. Usually, when we are dealing with metals or semiconductors, this thermoelectric term is neglected since, to develop a detectable temperature gradient ΔT

across its extremities, the sample should have a low thermal conductivity κ and a high Peltier coefficient. Also, in order that the thermoelectric term be comparable with the ohmic term, the electrical resistance, and thus the resistivity ρ, should be small. In other words the thermoelectric figure of merit (see Goldsmid 1964)

$$Z = \alpha^2/\kappa\rho \tag{24}$$

should be high in order to have a significant contribution from the thermoelectric term. It was found that in bismuth this is the case (Issi *et al.* 1971) and the effect is rather large. Even in the cases of arsenic (Jeavons and Saunders 1969; Heremans *et al.* 1977) and antimony (Oktü and Saunders 1967*a*) special care was needed to perform electrical measurements under strict isothermal conditions in certain temperature ranges.

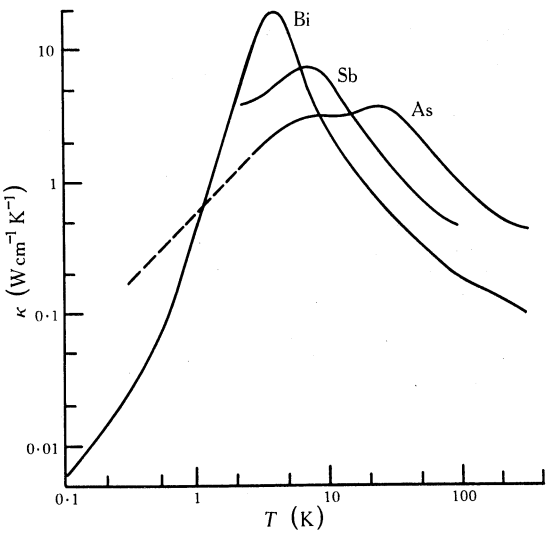

Fig. 8. Typical behaviour of the thermal conductivity κ of the group V semimetals as a function of temperature. The three maxima, which are those of κ_L, lie around 3·5, 8 and 30 K for bismuth, antimony and arsenic respectively, the Debye temperatures being 120, 200 and 282 K. Note that in the higher temperature range where κ_E dominates in antimony and arsenic, and is important in bismuth, the thermal conductivity increases with increasing density of carriers as expected. The dashed part of the arsenic curve represents the recent ultralow temperature results of Uher (1978*b*), shifted upwards (cf. Fig. 11).

It is worth noting also that the residual resistivity ratio (RRR), which is used as a criterion of sample purity and crystalline perfection, must be modified for the case of bismuth. In metals and also in arsenic and antimony an RRR measurement reflects directly the mobility ratio for the two temperatures considered, generally 4·2 and 300 K. For bismuth, we have already seen that the size of the sample has a large influence on the RRR (Section 3*c*). In addition, the carrier density increases by about an order of magnitude from the liquid helium range up to room temperature. Thus, even in an infinite sample, if one wants to give the same meaning to the RRR as for metals, one should multiply this ratio by a factor of nearly 8.

4. Thermal Conductivity

Results for the thermal conductivity of bismuth single crystals in the liquid helium range were obtained by Shalyt (1944), while Rosenberg (1955) investigated a wider temperature range for polycrystalline antimony. The first comprehensive analysis was performed by White and Woods (1958) on their data for polycrystalline bismuth and antimony from 2 to 150 K. Although the essentials of our present understanding of the thermal conductivity of these materials is contained in the paper by White and Woods, there has been more work performed since then on well-characterized single crystal material. For bismuth, both components of the zero-field thermal conductivity $\kappa_{\parallel}$ and $\kappa_{\perp}$ have been reported for a wide temperature range (Gallo *et al.* 1963; Kuznetsov *et al.* 1970; Pratt and Uher 1978) while, for antimony, only $\kappa_{\parallel}$ has been measured from 2 to 100 K (Red'ko *et al.* 1970) and from 0·05 to 5 K (Pratt and Uher, personal communication). For arsenic, the first measurements were reported for $\kappa_{\perp}$ by Heremans *et al.* (1977) from 2 to 300 K, although Little (1926) had given the room temperature value for polycrystalline material. Uher (1978*b*) recently extended these measurements to ultralow temperatures.

Table 3. Heat transport mechanisms in materials below 300 K

Material	Lattice	Electrons, holes	Bipolar
Insulator	All temperatures	—	—
Semiconductor	All temperatures	Usually weak	—
Metal	—	All temperatures	—
Bismuth	2–20 K	Below 1 K, above 20 K	Above 50 K
Antimony	Low temperatures	All temperatures	Weak
Arsenic	Low temperatures	All temperatures	—

A typical behaviour of the thermal conductivity of the group V semimetals below room temperature is represented in Fig. 8, while Table 3 shows how most of the known low temperature heat transport mechanisms compete to yield the total thermal conductivity of these materials. Indeed, we are in a unique situation here to review these various mechanisms since in other materials, like pure metals and insulators, there is usually only one type of conductivity that is predominant.

Generally speaking, in a given direction, the total thermal conductivity κ is the sum of the electronic κ_E and lattice κ_L contributions:

$$\kappa = \kappa_E + \kappa_L . \tag{25}$$

Only at temperatures higher than room temperature do other processes start to contribute significantly. In bismuth (Korenblit *et al.* 1970; Uher and Goldsmid 1974*b*) and antimony single crystals (Red'ko *et al.* 1970), the total thermal conductivity has been separated into its electronic and lattice components by applying a magnetic field at intermediate temperatures. This was also done recently for arsenic (Uher 1978*b*), antimony (Pratt and Uher, personal communication) and bismuth (Pratt and Uher 1978) at ultralow temperatures. In contrast to metals, the magneto-resistances of these semimetals, and especially bismuth, are very large, and so will be their magnetothermal resistance. Thus only relatively moderate magnetic fields are needed to reduce the electronic component to insignificance, provided the temperature is not too high.

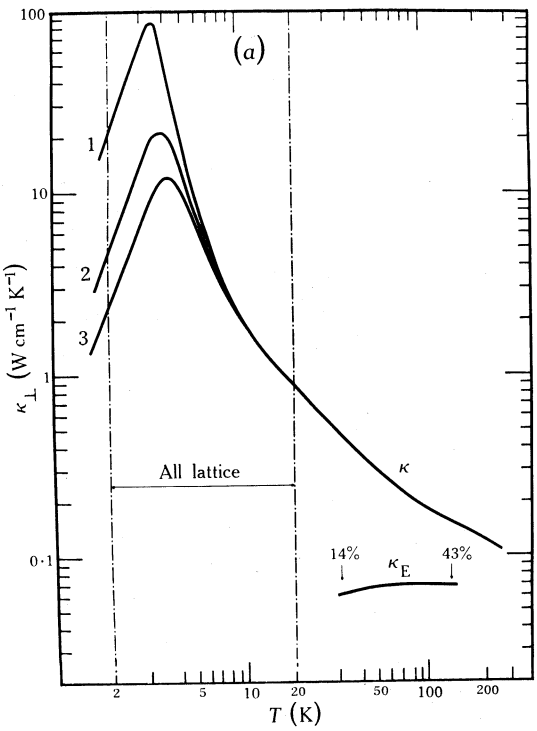

Fig. 9. Temperature variation of the thermal conductivity of bismuth:

(*a*) Results from Issi and Mangez (1972) and Boxus and Issi (1977) for three binary samples of different cross sections cut from the same ingot: sample 1, $8{\cdot}8\times8{\cdot}6$ mm^2; sample 2, $3\times2{\cdot}8$ mm^2; sample 3, $3\times1{\cdot}2$ mm^2. In the range from 2 to 20 K the lattice thermal conductivity is the sole mechanism and the dielectric size effect is clearly demonstrated. The curve representing the total electronic thermal conductivity κ_E at higher temperatures, as determined by Uher and Goldsmid (1974*b*), shows that κ_E amounts to 14% of the total thermal conductivity at 35 K and 43% at 150 K.

(*b*) Ultralow temperature measurements from Pratt and Uher (1978) for four samples: sample 2, a cylindrical bisectrix sample of 0·23 cm diameter; sample 4, a polycrystal of 0·44 cm diameter; sample 5, a cylindrical sample of 0·43 cm diameter with its axis inclined by 79° to the trigonal axis; sample 6, a trigonal sample of $0{\cdot}2\times0{\cdot}4$ cm^2 cross section. The dashed line represents T^3 behaviour. The solid curve is explained in the paper by Pratt and Uher.

The results for bismuth confirmed the findings of White and Woods (1958), showing that, in the range 2–20 K, the thermal conductivity is purely lattice and that the relative contribution of κ_E increases with increasing temperature. The data for single crystals shown in Fig. 9 indicate that κ_E amounts to 14% of the total thermal conductivity at 35 K and 43% at 150 K. For antimony, the carrier density is sufficiently high at all temperatures to maintain κ_E comparable with κ_L (Fig. 10). Also, it is usually assumed that the high carrier density is mainly responsible for phonon scattering. In arsenic, the two contributions have been tentatively computed

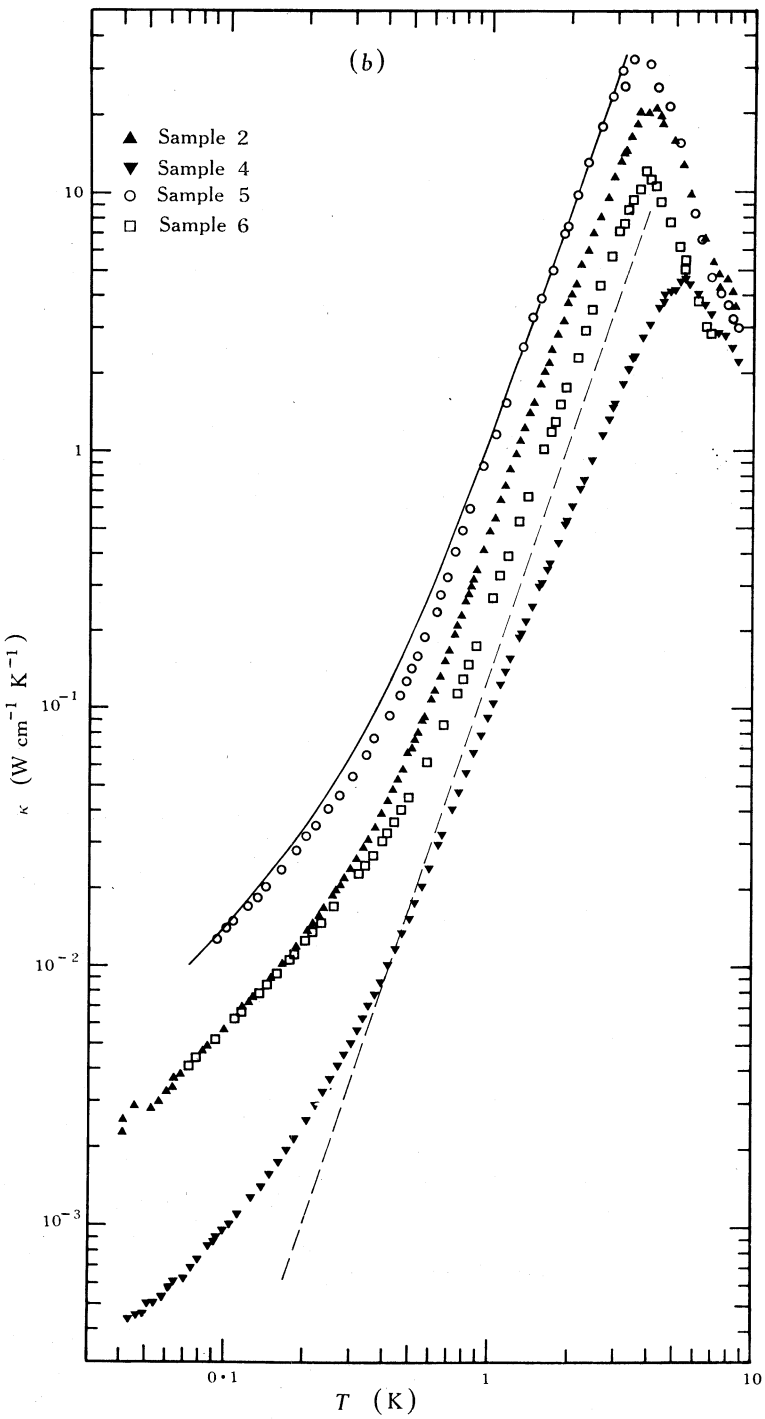

Fig. 9*b* [see caption on facing page]

(Fig. 11) and it seems that the behaviour is quite similar to that of antimony. Because the magnetoresistance of arsenic is much smaller than for bismuth, κ_E and κ_L have only been experimentally separated at very low temperatures (Uher 1978*b*). At intermediate temperatures very high magnetic fields would be needed to do this.

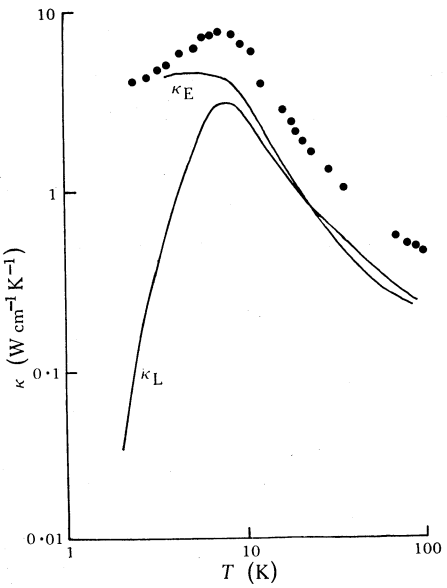

Fig. 10. Temperature variation of the thermal conductivity of antimony (from Red'ko *et al.* 1970). The plotted points represent the total measured conductivity, while κ_E and κ_L are the electronic and lattice contributions respectively, separated by means of a magnetic field.

(*a*) *Electronic thermal conductivity*

The Wiedemann–Franz law states that the electronic thermal conductivity κ_i due to a group of charge carriers i, where i refers to electrons or holes, is proportional to the electrical conductivity σ_i at a given temperature, that is,

$$\kappa_i = L_i T \sigma_i, \tag{26}$$

where L_i is the Lorenz number, which for a free electron system takes the value

$$L_0 = \tfrac{1}{3}\pi^2 (k_B/e)^2 = 2{\cdot}44 \times 10^{-8} \quad \mathrm{V^2\,K^{-2}}. \tag{27}$$

This law supposes that the charge carriers are highly degenerate and that the same relaxation time may be ascribed to both the electrical and electronic thermal conductivities. The first condition is naturally satisfied in metals, and should hold

---

Fig. 11. Temperature variation of the thermal conductivity of arsenic:

(*a*) Results from Heremans *et al.* (1977) for a binary sample. The plotted points represent the measured data. The electronic thermal conductivity κ_E was computed from electrical conductivity data by means of the Wiedemann–Franz law. At higher temperatures a small correction was made to account for the slight departure of the charge carrier system from total degeneracy. The lattice thermal conductivity κ_L was obtained by subtracting κ_E from the measured total conductivity; κ_L has a maximum around 30 K.

(*b*) Ultralow temperature measurements from Uher (1978*b*) performed on a sample of different residual resistivity ratio from that of (*a*).

Note the different scales on the κ axes in (*a*) and (*b*).

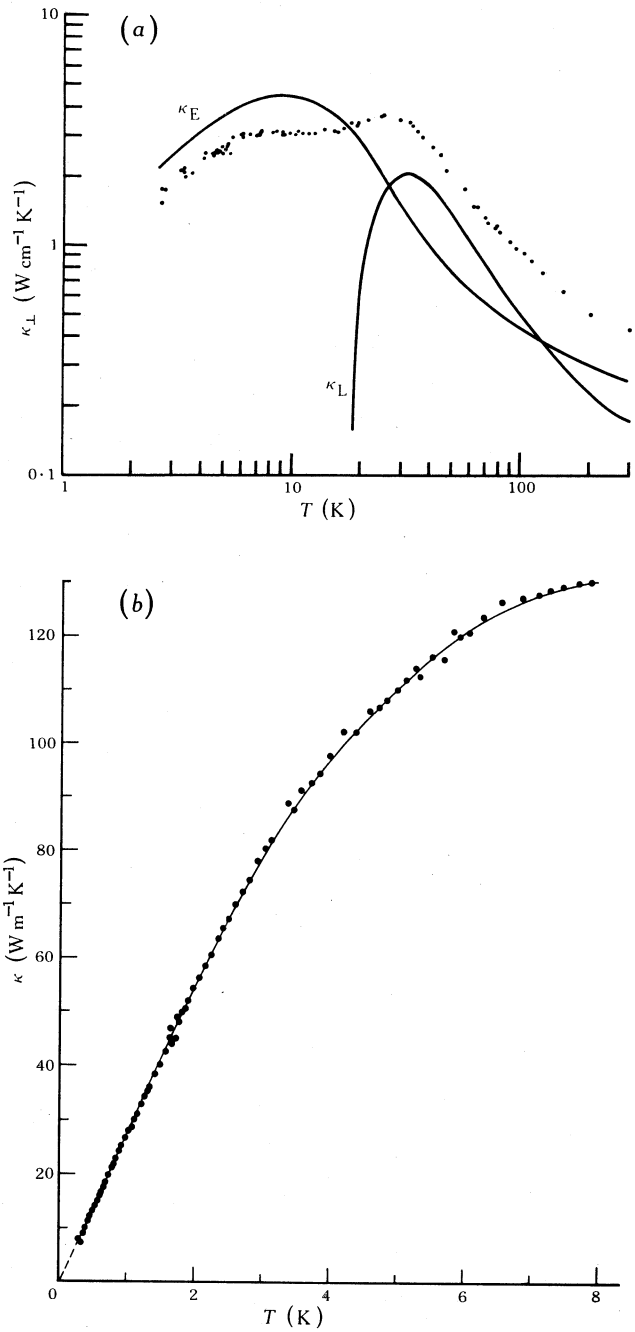

Fig. 11 [see caption on facing page]

reasonably for arsenic and antimony, provided small corrections are applied. However, for bismuth this condition is expected to hold only at lower temperatures, while at higher temperatures the Lorenz number should be expressed differently, in a way analogous to semiconductors, to account for the fact that the charge carriers are not totally degenerate. The second condition is fulfilled in metals only for some temperature ranges. The reason is that, while electron–phonon large angle scattering is as effective in reducing both conductivities, small angle scattering is much more effective in reducing the electronic thermal conductivity than the electrical conductivity. This is a consequence of the well-known fact that a thermal gradient affects the Fermi distribution in a different way from an electric field. Thus, for metals below the Debye temperature, when large angle scattering begins to be less probable than low angle scattering, the Wiedemann–Franz law is no longer valid. At sufficiently low temperatures where impurity scattering, which is essentially elastic, dominates, the law holds again. Fortunately, this complication is expected to occur in semimetals only at very low temperatures. Because of their small Fermi surfaces, the charge carriers suffer large angle scattering until the effective temperature θ^* (equation 18) is reached, and above θ^* the Wiedemann–Franz law should hold provided the charge carriers are fully degenerate and intravalley scattering dominates.

Further, in semimetals, as is the case for intrinsic semiconductors, electrons and holes may participate independently in heat transport as two monopolar contributions κ_e and κ_h from electrons and holes, or in pairs as a bipolar contribution κ_{eh}. For partial Lorenz numbers L_e and L_h, the Wiedemann–Franz law takes the form (26) with (Harman and Honig 1967; Blatt 1968)

$$L_i = (k_B/e)^2\{I_1(\eta_{Fi})\, I_3(\eta_{Fi}) - I_2^2(\eta_{Fi})\}/I_1^2(\eta_{Fi}), \tag{28}$$

where

$$\eta_{Fi} = \varepsilon_{Fi}/k_B T \tag{29}$$

is the reduced Fermi energy and

$$I_j(\eta_F) = \int_0^\infty \eta^j (-\partial f_0/\partial\eta)\, \mathrm{d}\eta, \tag{30}$$

f_0 being the Fermi–Dirac distribution function. The bipolar term is given by

$$\kappa_{eh} = T\{\sigma_e \sigma_h/(\sigma_e+\sigma_h)\}\,(\alpha_h-\alpha_e)^2, \tag{31}$$

where σ_e and σ_h are the partial electrical conductivities of electrons and holes, and α_e and α_h are the partial thermopowers, which will be defined in Section 5*a*(i). The total electronic conductivity is then

$$\kappa_E = \kappa_e + \kappa_h + \kappa_{eh}. \tag{32}$$

In the case of partially degenerate systems, when the carriers have a parabolic dispersion, if it is assumed that the relaxation time is expressed as in equation (19) (pure acoustic intravalley phonon scattering), the relation (28) reduces to (Heremans *et al.* 1977)

$$L_i = \tfrac{1}{3}(k_B/e)^2\{\pi^2 - \tfrac{1}{3}\pi^4(k_B T/\varepsilon_{Fi})^2\}. \tag{33}$$

Equation (33) was used by Heremans *et al.* for arsenic and is applicable in principle to antimony, though there has not yet been a detailed analysis carried out for the thermal conductivity of this material. The relation (33) is also expected to hold for holes in bismuth at intermediate temperatures. Note that $(k_B T/\varepsilon_{Fi})^2$ is a correction term, which takes into account the departure from full degeneracy at higher temperatures. For arsenic, this term will be negligible at low temperatures and will reach a few per cent at room temperature, while for antimony it is expected to be larger. The bipolar term of the electronic thermal conductivity may also be neglected at low temperatures, and it amounts to a few per cent of the total electronic thermal conductivity around room temperature for arsenic (Heremans *et al.* 1977) and should be larger in antimony (Red'ko *et al.* 1970).

In bismuth at low temperatures, an expression for the Lorenz number of electrons may be derived, taking into account the non-parabolicity in the framework of the Heremans and Hansen (1979) pseudoparabolic model. However, at higher temperatures, even when the valence band is assumed to be rigid and parabolic, we cannot make the second-order approximation as in equation (33) but must use instead the complete analytical formulae (Gallo *et al.* 1963). In the case of the conduction band of bismuth, the situation is even worse, as could be expected, since we must take into account not only the non-parabolicity but also the temperature variation of the band parameters.

If we look now at the experimental results, we may see that for arsenic, in the range where impurity scattering predominates and the carrier system is fully degenerate, one might have expected to find the Sommerfeld value for the Lorenz number L_0. However, Heremans *et al.* (1977) found a value of $0{\cdot}75\,L_0$. This is not in contradiction with the recent findings of Uher (1978*b*), who reports a constant Lorenz number below 2 K which is equal within 4% to L_0. Above 2 K, however, L decreases continuously to reach a value of about $0{\cdot}75\,L_0$ at 7 K. For bismuth at ultralow temperatures, the total thermal conductivity tends towards a linear temperature dependence (Fig. 9*b*). This shows that, as expected, the electronic thermal conductivity should predominate at sufficiently low temperatures. The Lorenz number was found to be almost equal to the Sommerfeld value L_0 (Pratt and Uher 1978). Above the dielectric maximum the Lorenz numbers for bismuth (Uher and Goldsmid 1974*b*) and antimony (Red'ko *et al.* 1970) have been found to deviate appreciably from L_0.

At higher temperatures, because of the probable onset of intervalley scattering, which is essentially inelastic, a deviation from L_0 is expected to be found in all three semimetals. However, this has not yet been verified experimentally. Because of the decreasing magnetoresistance with increasing temperature, very high magnetic fields are needed at high temperatures to separate the electronic and lattice components of the observed total thermal conductivity.

We note that, roughly speaking, the results for the electronic thermal conductivity of the group V semimetals are consistent with the main features of their electronic properties. Arsenic, which has the highest electronic population at all temperatures, exhibits an almost metallic behaviour with the highest κ_E. At the other end of the scale, because of the low carrier density in bismuth, its κ_E is only significant in the lowest and highest temperature ranges and is smaller than in arsenic. For antimony, κ_E is situated between these two extremes.

(*b*) *Lattice thermal conductivity*

The Debye relation is widely used in the discussion of the lattice thermal conductivity of electrical insulators. If c_v is the lattice specific heat at constant volume, l the phonon mean free path and v_s the velocity of sound in the solid, then

$$\kappa_L = \tfrac{1}{3} c_v v_s l. \tag{34}$$

In the case of bismuth from 2 to 20 K, we are in the most spectacular range of the Debye relation in which both c_v and l vary drastically with temperature (Figs 8 and 9). Below the dielectric maximum, an almost T^3 dependence is observed, which reflects that of the lattice specific heat in this temperature range. The mean free path is constant and equal, within a numerical factor of the order of unity, to a transverse dimension of the sample. The velocity of sound is almost independent of temperature. Above the dielectric maximum the lattice thermal conductivity first decreases very rapidly with increasing temperature and then starts an almost linear decrease with temperature, which is characteristic of the high temperature phonon–phonon umklapp processes.

For antimony, there is no temperature region where κ_L is the sole mechanism. However, its contribution has been experimentally estimated. The high carrier density, which is responsible for the important electronic contribution κ_E, also reduces κ_L via phonon–electron scattering, which becomes the predominant scattering mechanism below the dielectric maximum and leads to the observed T^2 variation (Fig. 10).* This was shown by White and Woods (1958) and further extended to lower temperature on single crystals by Blewer and Zebouni (1966), who found that this T^2 law holds down to 0·4 K. The maximum is also less pronounced than in the case of bismuth and the higher temperature T^{-1} variation characteristic of phonon–phonon umklapp processes was observed by White and Woods (1958).

For arsenic, we may tentatively say that κ_L has a similar behaviour to that in antimony, with a dielectric maximum around 30 K (Fig. 11). Below this maximum, phonons are probably mainly scattered by the charge carriers and, above, by other phonons. Note that Uher (1978*b*) was able to detect a small lattice contribution below 5 K, which was found to be proportional to T^2.

It is interesting to note that the lattice contributions have a maximum around 3·5 K for bismuth, 8 K for antimony and 30 K for arsenic, while the Debye temperatures for these materials are 120, 200 and 282 K respectively. This is in qualitative agreement with the predictions of the Debye theory.

(i) *Low Temperature Size Effects*

Since below about 20 K the thermal conductivity of bismuth exhibits the typical dielectric behaviour, one would expect that, around and below the dielectric maximum, the magnitude of the thermal conductivity would be very sensitive to the size of the specimen. The range of temperatures where this is likely to occur is known as the Casimir range (Casimir 1938; Herring 1954*a*). When the temperature decreases, the mean free path of the thermal phonons for umklapp processes increases exponentially. At low temperatures, it will eventually become comparable with the geometrical dimensions of the sample, which usually has typical transverse dimensions of a few millimetres.

* See, however, note added in proof (at end of paper).

It was already apparent in the work of White and Woods (1958), performed on bismuth polycrystals, that single crystal samples with cross sections of a few square millimetres would show size effects in the liquid helium range. Issi and Mangez (1972) and Kopylov and Mezhov-Deglin (1974) showed that in single crystal material the thermal conductivity in the T^3 regime was indeed proportional to the transverse dimensions of the specimen. The samples compared by Issi and Mangez (1972) consisted of two legs of different thicknesses of a tuning fork. This enabled a comparison of two specimens of the same purity, crystal perfection and thermal and mechanical history. Further, it appeared from their results that the size effect would probably persist above the Casimir range. This would be consistent with Herring's (1954*a*) prediction that lower energy phonons than the thermal ones might contribute significantly to the thermal conductivity, especially in rhombohedral crystals. Recently, this prediction was experimentally confirmed for bismuth on two tuning fork samples by Issi *et al.* (1976).

(ii) *Intermediate Temperature Size Effects*

In order to understand the contribution of low energy phonons to the lattice thermal conductivity one should artificially divide the phonons into two classes (Herring 1954*a*):

Class 1. The low energy subthermal phonons with wave numbers $q < q_c$, where the energy corresponding to q_c is approximately equal to $0{\cdot}1\,k_B T$ at temperatures below the Debye temperature (in bismuth $\theta_D = 120$ K). To these phonons, we associate a single-mode relaxation time (Klemens 1951) given by the asymptotic relation (Herring 1954*a*)

$$\tau^{-1}(q) = A\,q^{\beta}\,T^{5-\beta}. \tag{35}$$

Class 2. The higher energy phonons which are those with wave number $q > q_c$ and thermal conductivity $\kappa(q>q_c)$. Thus the total lattice thermal conductivity will be given by

$$\kappa = \kappa(q>q_c) + (k_B v_s^2/6\pi^2)\int_0^{q_c} \tau(q)\,q^2\,\mathrm{d}q, \tag{36}$$

where v_s is the velocity of sound, which we suppose to be independent of energy.

According to Herring (1954*a*), $\beta = 3$ for longitudinal phonons in a rhombohedral material. Using this value and introducing $\tau(q)$ from equation (35) into (36), we find for two arms of thicknesses W_1 and W_2 of the tuning fork ($W_1 > W_2$)

$$\Delta\kappa = \kappa_1 - \kappa_2 = (k_B v_s^2/18\pi^2 A T^2)\ln(W_1/W_2), \tag{37}$$

where we have assumed $\kappa(q>q_c)$ to be unaffected by size (Issi *et al.* 1976). Thus, if the detected size effect were to be ascribed to the subthermal low energy phonons, one should find a T^{-2} variation of $\Delta\kappa$. This is what was observed in the intermediate temperature range for two tuning fork samples by Issi *et al.* (1976). Also, from the observed T^{-2} curves, and taking $v_s = 2{\cdot}55\times10^5$ cm s^{-1} in the binary direction, they found an experimental value for A of 39×10^{-17} cm^3 s^{-1} K^{-2} for both samples.

Note that the relatively large contribution of low energy phonons to the total lattice thermal conductivity is due to the q^{-3} dependence of the relaxation time of

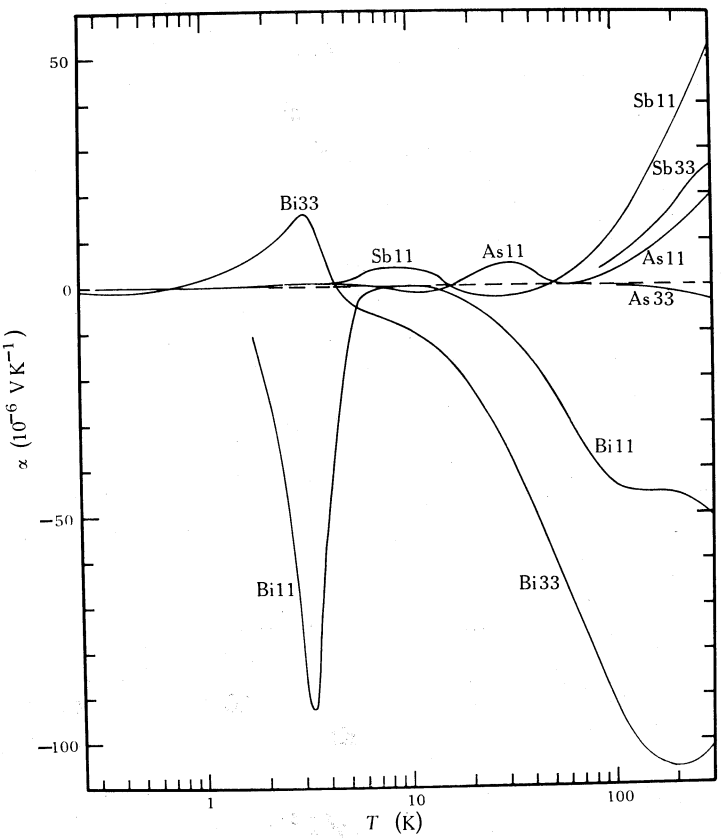

Fig. 12. Temperature dependence of the thermopower α of the three group V semimetals. The indices 11 and 33 denote the binary ($\perp$) and trigonal ($\parallel$) directions respectively. The sources of the data and the corresponding temperature ranges are set out below.

Semimetal	α	T range (K)	Reference
As	α_{11}	2·6–300	Heremans *et al.* (1977)
	α_{11}	0·3–7·6	Uher (1978*b*)
	α_{33}	80–300	Jeavons and Saunders (1970)
Sb	α_{11}	80–300	Saunders and Oktü (1968)
	α_{11}	3·3–300	Red'ko and Shalyt (1968)
	α_{33}	80–300	Saunders *et al.* (1965)
Bi	α_{11}	80–300	Gallo *et al.* (1963)
	α_{11}	1·8–100	Boxus and Issi (1977)
	α_{11}	0·04–3	Uher and Pratt (1978)
	α_{33}	80–300	Gallo *et al.* (1963)
	α_{33}	0·04–3	Uher and Pratt (1978)
	α_{33}	2·5–80	Korenblit *et al.* (1969)

these phonons. This q^{-3} dependence, which is a characteristic of rhombohedral structure, has important consequences when compared with the less pronounced q^{-2} dependence expected for cubic materials. It should explain too the large phonon-drag effects found in the group V semimetals and especially in bismuth (see Section 5*b*).

Also the experimental determination of the coefficient A enables us to compute the mean free path of the phonons interacting with electrons, provided that the dimensions of the Fermi surface in k space are known.

5. Thermopower

In Fig. 12 the thermopowers $\alpha_{\parallel}$ and $\alpha_{\perp}$ of the three group V semimetals are shown as functions of temperature. In the lowest and highest temperature ranges there are regions where the thermopowers vary almost linearly with temperature, while in the intermediate region there are pronounced extrema. Usually in metals a linear behaviour is indicative of diffusion mechanisms, while low temperature humps are attributed to phonon-drag effects.

The first comprehensive analysis of the diffusion thermopower of a group V semimetal was performed by Gallo *et al.* (1963), on the experimental data they obtained for bismuth. This was followed by the extensive work of Saunders and Oktü (1968) on antimony and Jeavons and Saunders (1970) on arsenic. Low temperature phonon-drag humps were first observed by Kuznetsov and Shalyt (1967) in bismuth, Red'ko and Shalyt (1968) in antimony and Heremans *et al.* (1977) in arsenic.

We shall review successively the diffusion and the phonon-drag effects. For this latter mechanism, its effect on the electrical conductivity will also be briefly discussed.

(a) Diffusion thermopower

The diffusion thermopower is caused by the difference in the broadening of the region around ε_F in the Fermi distribution between different regions of the sample due to the thermal gradient. Diffusion usually takes place from hot to cold regions and is counterbalanced by the thermoelectric e.m.f. Fig. 13 gives a schematic representation of the difference between the thermal smearing in the semimetals and that which occurs in ordinary metals and semiconductors. It may be easily seen from this figure why the thermopower is so high in semiconductors ($\sim 10^{-3}\,\mathrm{V\,K^{-1}}$), so small in pure metals ($\sim 10^{-6}\,\mathrm{V\,K^{-1}}$) and takes an intermediate value in semimetals (10^{-5}–$10^{-4}\,\mathrm{V\,K^{-1}}$).

Before we derive quantitative expressions for the diffusion thermopower of group V semimetals it is worth briefly sketching the situation qualitatively. Firstly, as for the electrical and thermal conductivities one would expect to have anisotropic thermopowers. Then, as for the case of intrinsic semiconductors, at least two types of carriers should be taken into account. For arsenic and antimony, up to room temperature, since the carrier statistics are totally degenerate, one could predict a behaviour similar to that of ordinary metals. For bismuth, the non-parabolicity of the conduction band, effective at all temperatures, as well as the partial degeneracy of the carriers above say 60 K should give rise to a more complicated behaviour. In fact, the history of the analysis of the temperature dependence of the diffusion thermopower for bismuth is a long and tricky story. The first analysis of measurements made on good single crystals was carried out by Gallo *et al.* (1963) in the temperature range 80–300 K. Assuming parabolic rigid bands, and starting from their experimental values of $\alpha_{\parallel}$ and $\alpha_{\perp}$ and those of the mobility ratios, they were able to compute the partial thermopowers of electrons and holes (see equations (47) below). Then, assuming pure acoustic phonon scattering, and using equation (46), they were able to compute the

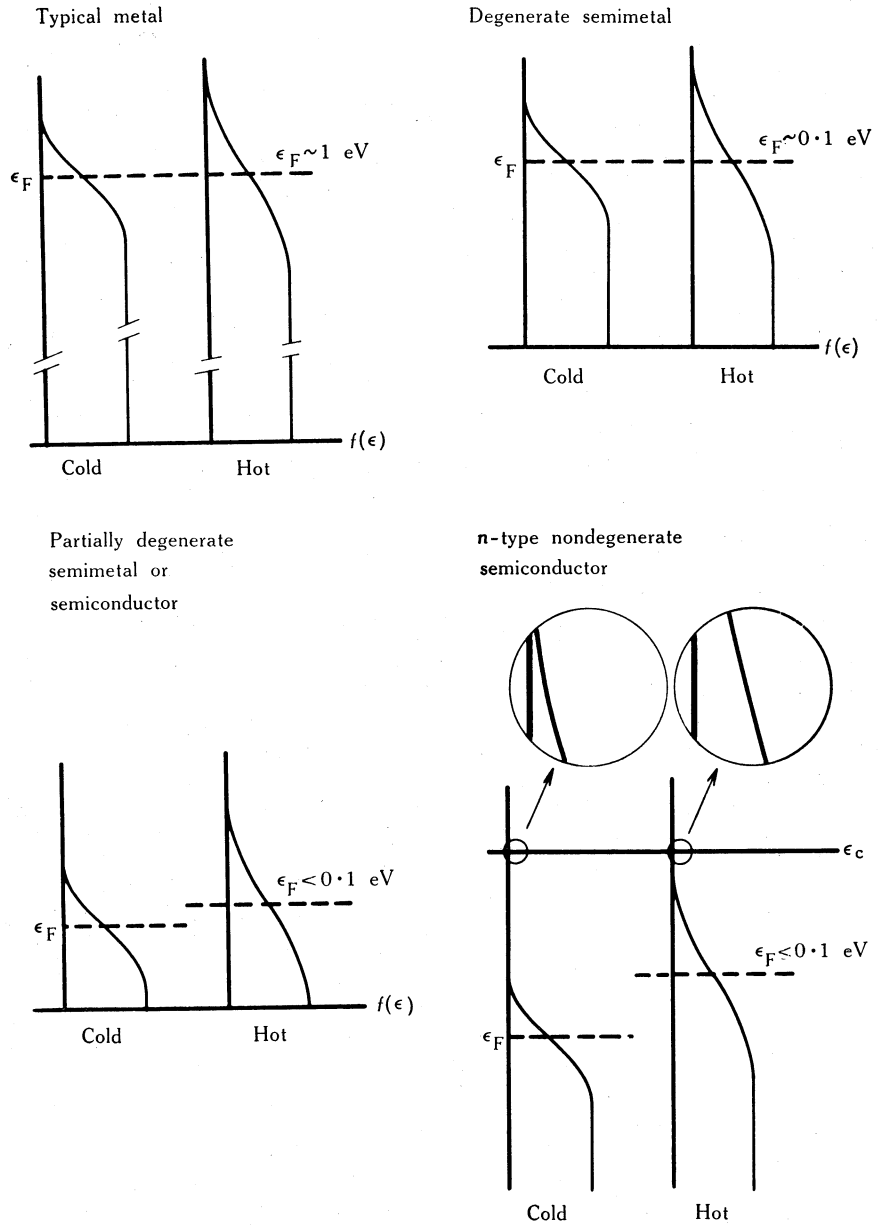

Fig. 13. Schematic representation of the principle of thermopower generation in different kinds of solids. For metals and totally degenerate semimetals, the thermoelectric voltage is due to the broadening of the Fermi–Dirac distribution with an almost constant Fermi level. However, since ε_F is much larger in a metal, for a given temperature the relative effect is much larger in a semimetal, and the thermopower is expected to be consequently larger in the latter. In a partially degenerate semimetal or semiconductor, or in a nondegenerate extrinsic semiconductor, there is a difference in ε_F between the cold and hot ends. Here also it may be seen that the relative effect is expected to be largest in a nondegenerate extrinsic semiconductor. The shift of the Fermi levels and the broadening of the distributions are both exaggerated for the sake of clarity.

Fermi energies for electrons and holes. Oddly enough, the agreement was quite good when these energies were compared with those obtained at 4·2 K by means of oscillatory quantum techniques. When the magnetoreflection measurements of Brown *et al.* (1963) clearly established the non-parabolicity of the electron band, the thermopower of bismuth was recalculated by Issi and Streydio (1967), using a non-parabolic dispersion for the conduction band. The results turned out to be inconsistent with the experimental findings. Later Hansen *et al.* (1978) analysed the thermomagnetic coefficients (including the zero-field ones) in terms of intravalley acoustic phonon scattering. They were able to obtain consistent results when all carriers were assumed to have a simple parabolic dispersion. Although this then confirmed and generalized the results of Gallo *et al.* (1963), the results could not be accepted since the analysis was based on a wrong assumption. For almost a decade, attempts to include the non-parabolicity via the density of states proved unsuccessful. However, very recently Heremans and Hansen (1979) were able to obtain good agreement below 80 K, by using their pseudoparabolic model (see Section 2*c*). The expressions describing their model were very like those used in the parabolic case.

(i) *Partial Diffusion Thermopowers*

Now let us compute the partial diffusion thermopowers for electrons and holes. By solving the Boltzmann equation (Harman and Honig 1967; Blatt 1968) we obtain the following expression for the partial thermoelectric power of electrons or holes:

$$\alpha_i = \pm(k_B/e)\{I_2(\eta_{Fi})/I_1(\eta_{Fi}) - \eta_{Fi}\}, \tag{38}$$

where the minus or plus signs refer to electrons or holes respectively. The transport integrals $I_j(\eta_{Fi})$ were recently derived by Heremans and Hansen (1979) in the most general case, i.e. in the framework of their pseudoparabolic model, and were expressed as

$$I_1(\eta_{Fi}) = F_0(\eta_{Fi}) + 2F_1(\eta_{Fi})/\eta_g, \tag{39a}$$

$$I_2(\eta_{Fi}) = 2F_1(\eta_{Fi}) + 3F_2(\eta_{Fi})/\eta_g, \tag{39b}$$

where the quantities $F_0(\eta_{Fi})$, $F_1(\eta_{Fi})$ and $F_2(\eta_{Fi})$ are the Fermi–Dirac integrals for the energy ε_{Fi} and

$$\eta_g = \varepsilon_g/k_B T \tag{40}$$

is the reduced direct energy gap between the band under consideration and any interacting band that may cause the non-parabolic dispersion.

It was also shown by Heremans and Hansen (1979) that for the pseudoparabolic model the relaxation time may be expressed as

$$\tau = \tau_0(\gamma/k_B T)^{-\frac{1}{2}}\gamma' \tag{41}$$

and, in the degenerate case, the partial diffusion thermopower is given by

$$\alpha_i = \pm\tfrac{1}{3}\pi^2(k_B/e)k_B T\gamma'_F/\gamma_F. \tag{42}$$

For degenerate parabolic bands, one may expand the transport integrals in series (Heremans *et al.* 1977) and obtain

$$I_1(\eta_{Fi}) \approx \eta_{Fi} \qquad \text{within 1\% for} \quad \eta_{Fi} > 3{\cdot}5 \tag{43a}$$

and

$$I_2(\eta_{Fi}) \approx \eta_{Fi}^2 + \tfrac{1}{3}\pi^2 \qquad \text{within 1\% for} \quad \eta_{Fi} > 3{\cdot}0. \tag{43b}$$

Equation (38) then reduces to

$$\alpha_i = \pm\tfrac{1}{3}\pi^2(k_B/e)\eta_{Fi}^{-1} \tag{44}$$

and we obtain, as expected, the expression used for ordinary metals (cf. Blatt 1968). Since the Fermi energies in group V semimetals are much smaller than those of ordinary metals, the partial thermopowers should be larger by roughly two orders of magnitude. For partially degenerate parabolic bands, the relaxation time for pure acoustic scattering is given by equation (19) and the transport integrals take the form

$$I_1(\eta_{Fi}) = F_0(\eta_{Fi}), \qquad I_2(\eta_{Fi}) = 2F_1(\eta_{Fi}), \tag{45}$$

which are the asymptotic forms of the integrals (39a) and (39b) for $\eta_g \to \infty$. The partial diffusion thermopower is then

$$\alpha_i = \pm(k_B/e)\big(2F_1(\eta_{Fi})/F_0(\eta_{Fi}) - \eta_{Fi}\big). \tag{46}$$

The expression (46) describes the thermopower of the holes in bismuth above 60 K and of the electrons and holes in antimony around and above room temperature. For the holes in bismuth below 60 K and the electrons and holes in antimony and arsenic below room temperature, equation (44) is a good approximation. For the electrons in bismuth, it was found that around 60 K equation (42) is applicable, and the main success of the Heremans and Hansen (1979) model was that, when this partial thermopower was combined with that of holes through equation (46), excellent agreement was obtained with the experimental results. At higher temperatures, the variation of the band parameters with temperature, which is not yet known precisely, renders the analysis of the results more speculative for bismuth.

(ii) *Total Diffusion Thermopower*

When more than one type of carrier is acting simultaneously, the total thermopowers $\alpha_\parallel$ and $\alpha_\perp$ may be computed on the assumption that the partial contributions act as e.m.f.'s in parallel:

$$\alpha_\parallel = \sum_i \left(\frac{\sigma_{\parallel i}\alpha_i}{\sum_i \sigma_{\parallel i}}\right), \qquad \alpha_\perp = \sum_i \left(\frac{\sigma_{\perp i}\alpha_i}{\sum_i \sigma_{\perp i}}\right), \tag{47}$$

where $\sigma_{\parallel i}$ and $\sigma_{\perp i}$ are the partial contributions of a band to the total electrical conductivity in the direction considered. It is worth noting that even in anisotropic crystals the α_i's for the diffusion thermopower are scalars, provided that the dependence of the relaxation time on momentum is assumed to be isotropic, while the σ_i's are not, and thus it is the partial conductivities that determine the anisotropy of the total diffusion thermopower.

(*b*) *Phonon-drag effects*

The principle of phonon-drag effects may be understood from simple arguments. Most of the transport theory is derived assuming Bloch conditions, i.e. that the phonon system is in equilibrium and that the electron system may be treated independently. This is certainly not rigorously the case when thermoelectric effects are considered, since a nonzero temperature gradient is assumed and lattice thermal conductivity takes place. However, in most cases when there is no strong coupling between the electron and phonon systems, the approximation is fair. This is not applicable at low temperatures, where there might be a significant coupling between these two systems and, as a consequence, an anisotropic transfer of momentum from one system to the other is likely to occur, resulting in a drag on the electrons. This extra electronic motion, which should be distinguished from the spontaneous diffusion discussed in the case of the diffusion thermopower, requires an additional thermoelectric field to counterbalance it, giving rise to the phonon-drag or lattice thermopower α_g. Conversely, when an electrical current flows in a solid, the electrons may drag along the phonons under certain conditions. This might result in an enhancement of the electrical conductivity.

We have already seen, while discussing the electrical conductivity (Section 3*a*), that in semimetals not all the phonons are likely to interact with the charge carriers. Energy and momentum conservation restrict the interactions to those with the low energy phonons. These interacting phonons are, in momentum space, confined in ellipsoids with semi-axes of twice the length of the semi-axes of the Fermi ellipsoids. This should apply in both senses: for phonons dragging electrons and vice versa.

(i) *Phonon-drag Thermopower*

Along the lines developed by Herring (1954*b*), Korenblit (1969) worked out a theory to explain the phonon-drag effects observed in the thermopower of bismuth. For $k_B T \ll \varepsilon_F$, he derived the following expression for the partial phonon-drag thermopower matrix element $(k\,l)$ experienced by carriers of group i:

$$\alpha_{g,i} = \frac{1}{e_i n_i (k_B T)^2} \sum_{a=1}^{3} \int_{\Omega_i} \frac{d^3q \exp(\hbar\omega_q^a / k_B T)\, \hbar\omega_q^a}{(2\pi\hbar)^3 \{\exp(\hbar\omega_q^a / k_B T) - 1\}^2} \frac{\tau^a(q)}{\tau_i^a(q)} v_l^a q_k , \tag{48}$$

where e_i and n_i are the charge and concentration of the ith carrier group, a is the phonon acoustic branch polarization number, v_l^a is the lth component of the group velocity of these phonons, $\tau_i^a(q)$ is the relaxation time of these phonons with carriers of group i, and $\tau^a(q)$ is the total relaxation time of these phonons, including that for boundary scattering. The integration is carried out for the phonon ellipsoid interacting with carriers of group i.

In contrast to the case of diffusion, the phonon-drag partial thermopowers are anisotropic and may be expressed by tensors. For bismuth, in terms of the crystallographic axes, these tensors for electrons and holes take the form (we shall omit hereafter the subscript g)

$$\begin{bmatrix} \alpha_{e11} & 0 & 0 \\ 0 & \alpha_{e22} & \alpha_{e23} \\ 0 & \alpha_{e32} & \alpha_{e33} \end{bmatrix}, \qquad \begin{bmatrix} \alpha_{h11} & 0 & 0 \\ 0 & \alpha_{h22} & 0 \\ 0 & 0 & \alpha_{h33} \end{bmatrix}. \tag{49}$$

These partial thermopowers should, as for the diffusion case, be weighted with the partial electrical conductivities

$$(\sigma_e+\sigma_h)\alpha = \sigma_e\alpha_e + \sigma_h\alpha_h . \tag{50}$$

For each valley of the Fermi surface, the temperature dependence of the effect may be imagined as follows. For temperatures below θ^*, only the phonon modes which may interact with the carriers will be populated, and strong phonon drag is expected to occur. The thermopower should then be proportional to T^3 like the lattice specific heat. For temperatures above θ^*, higher energy phonon modes will also be excited, and these phonons are not allowed to interact with electrons. However, these higher energy modes will effectively scatter the lower energy phonon modes, and we shall represent this scattering probability by the relaxation time $\tau^a_{pp}(q)$. The ratio $\tau^a(q)/\tau^a_i(q)$ is a weighting factor which represents the probability of a low energy phonon interacting with the electron as compared with that of all scattering processes. For an ideally perfect and infinite crystal, we have

$$\{\tau^a(q)\}^{-1} = \{\tau^a_{pp}(q)\}^{-1} + \{\tau^a_i(q)\}^{-1} . \tag{51}$$

Impurities and grain or crystal boundaries may also scatter the low energy phonons in a real crystal, and to each scattering mechanism m a corresponding relaxation time $\tau^a_m(q)$ may be associated. Thus we may more generally write

$$\{\tau^a(q)\}^{-1} = \sum_m \{\tau^a_m(q)\}^{-1} . \tag{52}$$

A quantitative comparison between theory and experiment in the case of bismuth is, for the time being, almost impossible because of all the adjustable parameters, of which little is known. For example, the only method at hand now to discriminate between electrons and holes in dragging effects is to carry out experiments on doped samples (Korenblit *et al.* 1969). However, these experiments have serious drawbacks if we want to reach quantitative conclusions. Doping introduces new scatterers to low energy phonons, as well as to electrons and holes. Besides the main effect of doping being to alter the Fermi energies of the carriers, it also leads to interaction with phonon modes quite different from the drag phonons in intrinsic material. So the analysis of results on doped material might prove even more complicated.

However, some of the observed effects may be qualitatively interpreted. The extreme sensitivity of phonon drag to size in bismuth binary single crystals has been recently demonstrated by Boxus and Issi (1977). They found that the magnitude of the peak of the phonon-drag thermopower can be swept from almost -10^{-4} to $+10^{-5}\,\mathrm{V\,K^{-1}}$ by reducing a transverse dimension from 9 to 1·2 mm (Fig. 14). This means that decreasing the thickness enhances the relative contribution of the positive partial thermopower to the total one at the expense of the negative contribution. Their measurements suggested also that the phonon-drag hump is negative for an infinite binary sample, in contrast to the interpretation of all previous results. The data of Uher and Pratt (1978), which confirmed that this was true in the trigonal plane, were in good qualitative agreement with the experiments of Boxus and Issi

(1977). Since the measurements of Uher and Pratt (1978) were extended to ultralow temperatures they were able to observe two other peaks: a positive one around 1 K and a negative one around 0·4 K for $\alpha_\perp$. Oddly enough, Kopylov and Mezhov-Deglin (1974) found an increase in the magnitude of the positive phonon-drag

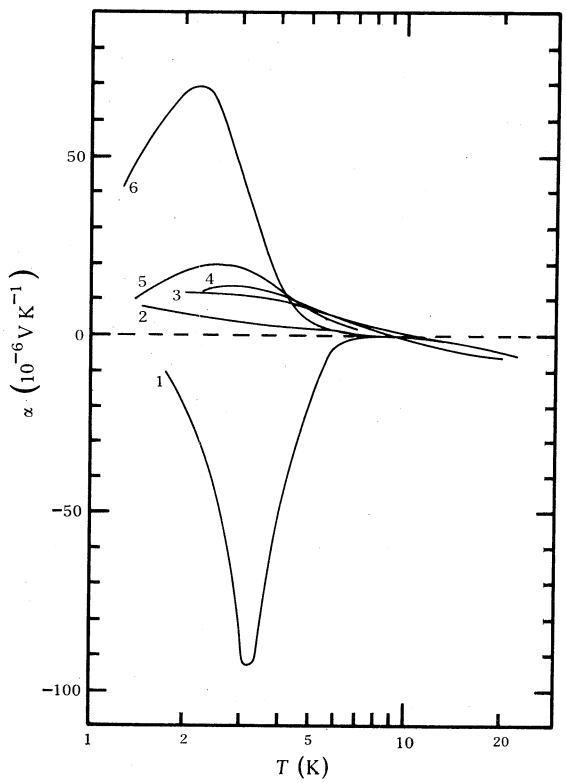

Fig. 14. Temperature variation of the thermoelectric power α of pure bismuth. Curve 1 shows the results from a sample with a rectangular cross section of $8{\cdot}8\times8{\cdot}6$ mm^2 (Boxus and Issi 1977), while curves 2 and 3 are from samples of rectangular cross sections $2{\cdot}8\times3{\cdot}0$ and $1{\cdot}2\times3{\cdot}0$ mm^2 respectively (Issi and Mangez 1972). Comparing these three samples (1–3) we see that the negative contribution to the total thermopower increases with increasing thickness at low temperatures. Curve 4 gives the results of Korenblit *et al.* (1969) from a cylindrical sample of diameter 2·0–3·0 mm. For curves 1–4, the sample axes are in the binary direction. Curves 5 and 6 show results from samples whose directions do not coincide with a principal crystallographic direction and which have almost circular cross sections of diameters 4·8 mm (5) and 7·5 mm (6) (Kopylov and Mezhov-Deglin 1974).

thermopower with increasing thickness on samples which were inclined by nearly 45° to the trigonal axis (Fig. 14). Preliminary measurements on trigonal samples (J. Boxus, unpublished data) indicate that size effects in this direction are probably not so important.

(ii) *Phonon Drag in Electrical Conductivity*

The occurrence of a possible enhancement of the electrical conductivity of metals at low temperatures due to phonon drag was foreseen by Klemens (1951), and later on worked out theoretically for the case of semiconductors by Goodman (1954) and Parrott (1957). Nowadays, there is a renewed interest in the subject and some authors have pointed to a possible effect of phonon drag on the electrical conductivity of metals at low temperatures (see e.g. Leavens and Laubitz 1975).

In the case of semiconductors, the effect expected ideally should be large at low temperatures. However, it is not possible to detect it experimentally, since in order to observe a significant effect the electron system must be degenerate (Goodman 1954). A degenerate semiconductor generally means a highly doped material, and thus dominant impurity scattering. Practically, this means that the probability for an electron to be scattered by a phonon is small compared with that of being scattered by an ionized impurity. For this reason semimetals, and particularly bismuth, are expected to be choice materials to observe such effects, since they are degenerate in their purest form and the phonons interacting with electrons have very large mean free paths (Section 4*b* (ii)).

Issi and Mangez (1972) showed that the size effects in the thermopower and the electrical conductivity, measured on the same samples, occur in the same temperature range, namely that in which the phonon-drag thermopower exhibits its maximum. One plausible explanation was to ascribe both size effects to the same mechanism. In the case of the electrical conductivity, the electrons dragging the phonons would cause a departure from equilibrium of the phonon system, resulting in an enhancement of the electrical conductivity. In the limit of strong phonon drag, the effective electron mean free path would become equal to that of the much larger low energy phonon mean free paths. The size effect observed in the electrical conductivity could then be an indirect observation of a phonon size effect. Although these observations are not conclusive, they suggest that the mean free path of the low energy phonons concerned should be considered in explaining the kind of size effects illustrated in Fig. 6. It might also explain the peculiar T^{-2} variation in certain temperature ranges.

6. Galvanomagnetic and Thermomagnetic Effects

We have already seen in Section 3 how pronounced are the galvanomagnetic effects in the group V semimetals and especially in bismuth. The same applies for their thermal equivalent, the thermomagnetic effects, which were discovered in bismuth by Ettingshausen and Nernst in 1886. However, in contrast to the case of galvanomagnetic properties, little was done on the thermomagnetic effects in the group V semimetals. Until this last decade, only a few scattered data existed in the literature. This was probably due in part to the fact that the thermal effects are more difficult to measure correctly than the electrical ones, and further that the low field thermomagnetic coefficients are more numerous than the galvanomagnetic ones. Thermomagnetic effects are also more difficult to interpret than the galvanomagnetic effects since, as is the case for the zero-field thermopower, there are two mechanisms which may contribute.

(*a*) *Galvanomagnetic effects*

For the A7 rhombohedral structure the generalized form of Ohm's law, which takes into account the anisotropy of the system and the presence of the magnetic

induction $\boldsymbol{B}$, should be considered. The theory of such effects has been reported with full details by many authors (Juretschke 1955; Abeles and Meiboom 1956; Drabble and Wolfe 1956; Okada 1957; Hartman 1969), and we shall only point out here the essential features. If $\boldsymbol{E}_i$ is the electric field and $\boldsymbol{J}_i$ the current density, the resistivity $\rho_{ij}(\boldsymbol{B})$ is given by

$$\boldsymbol{E}_i = \rho_{ij}(\boldsymbol{B})\, \boldsymbol{J}_j . \tag{53}$$

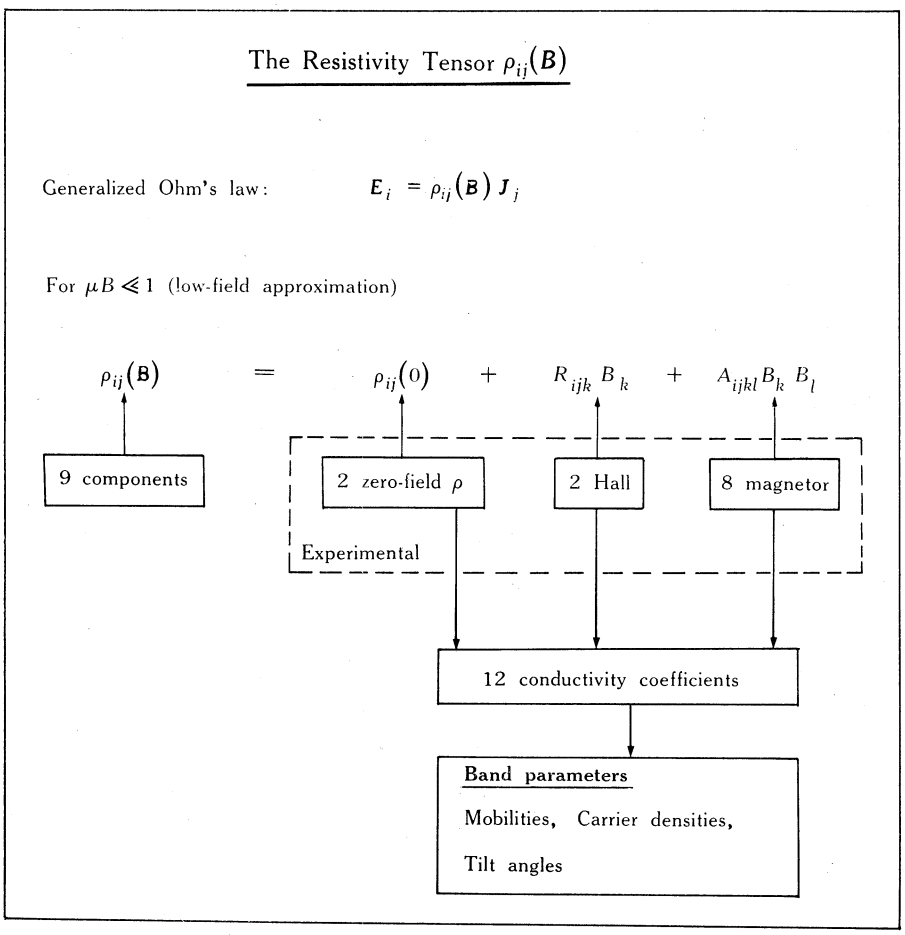

Fig. 15. Schematic representation of band parameter calculations from low-field galvanomagnetic measurements for a rhombohedral semimetal. (Note that 'magnetor' is used here as an abbreviation for magnetoresistance.)

In the limit of weak fields ($\mu B \ll 1$, where μ is a carrier mobility), only the terms in B and B^2 need be retained in the expansion of this tensor as a power series. Experimentally, 12 coefficients should be measured: 2 zero-field resistivities, 2 Hall coefficients and 8 magnetoresistance coefficients. Fig. 15 shows schematically how the band parameters are deduced from these coefficients.

Experimentally one has to turn to low-field measurements where the effects are very small. For bismuth, Zitter (1962) was the first to study rigorously this low-field condition in his investigation of the galvanomagnetic tensor of bismuth at 4·2 K. Hartman (1969) extended this work by carefully exploring the range 4·2–15·7 K. His results were consistent with the known Fermi surface. Abeles and Meiboom (1956) and Okada (1957) explored a higher temperature range. However, the data of Abeles and Meiboom were taken only at two fixed temperatures, 80 and 300 K, and those of Okada were taken at four temperatures from 113 to 318 K and all data were for fields above 200 Oe. More recently Michenaud and Issi (1972) investigated the temperature range from 77 to 300 K under strict isothermal conditions, rigorously satisfying the low-field condition. They were able to determine the temperature variation of the carrier density (Fig. 2), the tilt angle of the electron ellipsoids and the mobilities.

The two other group V semimetals were studied by the Durham group: antimony by Oktü and Saunders (1967*a*) and arsenic by Jeavons and Saunders (1969). They found interesting features of the Fermi surface and showed that carrier degeneracy was high and that its density remained almost independent of temperature up to 300 K; the carrier densities in antimony were found to vary from $3{\cdot}9\times10^{19}$ cm^{-3} at 77 K to $4{\cdot}2\times10^{19}$ cm^{-3} at 273 K, and in arsenic from $1{\cdot}9\times10^{20}$ cm^{-3} at 77 K to $2{\cdot}1\times10^{20}$ cm^{-3} at 305 K. For both semimetals an anomalous temperature variation of the mobilities was observed: $T^{-1{\cdot}4}$ for antimony and $T^{-1{\cdot}7}$ for arsenic instead of the expected T^{-1} variation.

Aubrey (1971) has expressed in a tractable form the conductivity tensor components as functions of band parameters, for an arbitrary value and a given direction of the magnetic induction. These relations, when used to determine band parameters, should in principle save a lot of experimental time since, at a given temperature, only one coefficient has to be measured as a function of magnetic field, and the problems associated with low-field measurements are almost eliminated. These expressions have been shown experimentally to describe certain components of the magnetoresistivity tensor of bismuth (Saunders and Sümengen 1972). Note also that Sümengen *et al.* (1974) were able to explain, at intermediate fields, the polar diagrams measured by Mase *et al.* (1962) at 20·4 K. In these measurements the magnitude of the intermediate magnetic field remains constant and the galvanomagnetic effects are measured as a function of its direction.

Galvanomagnetic measurements have also been used as a means of discrimination between the charge carriers. This has been the case for arsenic and antimony, where it was not known till recently which were the electron and hole pockets. Galvanomagnetic measurements on pure and tin-doped antimony led to the conclusion that in both cases holes were situated in the pockets with the larger tilt angle, which then allowed them to be located (Oktü and Saunders 1967*b*).

Using space–time symmetry restrictions for field-dependent tensors, Akgöz and Saunders (1975*a*, 1975*b*) were able to predict the measurable component for the transport effect of the group V semimetals and thus form the bases of the general description of the effects of a magnetic field on the transport properties. The field-dependent tensor method provides the theoretical basis for the description of transport properties in a magnetic field; it explains, for example, why the Umkehr effect occurs in those tensor components which have both odd and even contributions (see subsection (*b*) below).

(*b*) *Thermomagnetic effects*

If ∇T is the applied temperature gradient and $\boldsymbol{E}$ the resulting Seebeck field, the magnetothermopower tensor $\boldsymbol{\alpha}(\boldsymbol{B})$ is defined by

$$\boldsymbol{E} = \boldsymbol{\alpha}(\boldsymbol{B})\nabla T. \tag{54}$$

Grüneisen and Gielessen (1936) found that, for certain directions, when the magnetic field is reversed (a 180° rotation) the e.m.f. is not the same for both senses of the magnetic field. This effect, called the 'Umkehr' effect, was later remeasured by other authors for various configurations of $\boldsymbol{E}$, ∇T and $\boldsymbol{B}$ (Steele and Babiskin 1955; Smith and Wolfe 1966; Michenaud *et al.* 1970; Uher and Goldsmid 1974*a*). More recently Akgöz and Saunders (1975*b*), using field-dependent tensors, established the form of the thermomagnetic transport tensors and indicated for each crystallographic class, including the $\bar{3}m$, the components which contain an odd contribution.

If we expand in series the components $\alpha_{ij}(\boldsymbol{B})$ up to terms of second order in $\boldsymbol{B}$, we obtain 16 independent coefficients (Sümengen and Saunders 1972*a*) instead of the 12 found in galvanomagnetic effects. These 16 coefficients consist of the 2 zero-field coefficients $\alpha^0_{11} = \alpha^0_{22}$ and α^0_{33}, which were considered in Section 5 above and denoted for convenience by $\alpha_\perp$ and $\alpha_\parallel$ respectively; 4 coefficients for the linear terms, the so-called 'Nernst coefficients' α_{111}, α_{123}, α_{231} and α_{321}; and 10 coefficients for the quadratic terms, the so-called 'magneto-Seebeck coefficients'. The indices 1, 2 and 3 indicate the binary, bisectrix and trigonal directions respectively.

Michenaud *et al.* (1971) have measured three of the low-field coefficients, namely α_{231}, α_{3311} and α_{3322}, from 77 to 300 K and have shown that $\alpha_{23}(B_1)$ changes sign when going from low to intermediate fields. The same coefficients were measured by Hansen (1977) from 10 to 67 K and a change of sign was also observed for $\alpha_{23}(B_1)$. These observations were in disagreement with the expressions derived by Sümengen and Saunders (1972*b*)

$$\alpha_{ij}(\boldsymbol{B}) = \rho_{ik}(\boldsymbol{B})\{\alpha_e \sigma^e_{kj}(\boldsymbol{B}) + \alpha_h \sigma^h_{kj}(\boldsymbol{B})\}, \tag{55}$$

where α_e and α_h are the scalar partial diffusion thermopowers of electrons and holes respectively, ρ_{ik} is the total resistivity tensor component and σ^e_{kj} and σ^h_{kj} are the partial conductivity tensor components for electrons and holes respectively. Cheruvier and Hansen (1975) have shown that the partial thermopowers α_e and α_h, which are scalars at zero field (see Section 5*a*(i)), become tensors in a magnetic field if the Fermi surface is smeared and the relaxation time is energy dependent.

At low temperatures the thermomagnetic effects are very large (Korenblit *et al.* 1969; Tanuma *et al.* 1969) and cannot be explained in terms of a simple diffusion mechanism. Taking into account the anisotropy of bismuth, Korenblit (1969) developed a theory for the phonon-drag thermomagnetic effects which allowed the various components to be computed. This was based essentially on arguments developed earlier by Herring (1954*b*). However, the Korenblit theory does not explain all the low temperature experimental results. This is apparent from the work of Uher and Goldsmid (1974*a*), who showed also that a phonon-drag mechanism could persist up to the liquid nitrogen range. On the other hand, Jacobson and Ertl (1972) demonstrated that, if the electron density n_e is not rigorously equal to the

hole density n_h, one could observe relatively large discrepancies with the Korenblit theory. Also, in the temperature range where phonon-drag effects are predominant the size effects described in Section 5*b* might have a drastic influence on the thermomagnetic coefficients.

Analytical expressions for the 16 low-field phonon-drag thermomagnetic coefficients were systematically derived by Uher (1975). His formulae remain valid for the low-field diffusion thermomagnetic coefficients, provided the partial phonon-drag thermopower tensors are replaced by the scalar diffusion thermopowers (i.e. if the dispersion is assumed to be parabolic and the relaxation time to be energy independent).

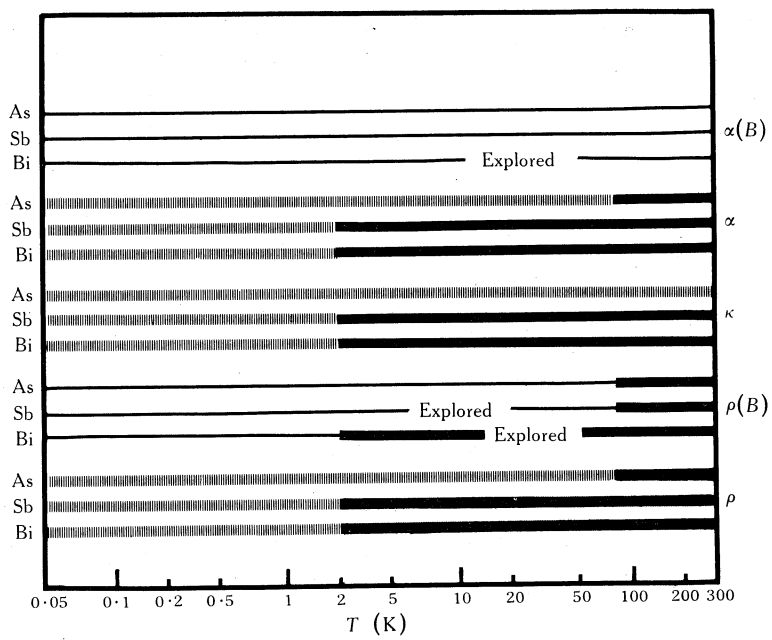

Fig. 16. Status of knowledge of the transport properties of the group V semimetals. The thick lines (solid and shaded) indicate the temperature ranges that have been fully investigated experimentally. This means that, for the magnetoresistivity tensor $\rho(B)$ and the thermomagnetic tensor $\alpha(B)$, all the components have been measured on single crystals and analysed in terms of band parameters. For the zero-field resistivity ρ, thermal conductivity κ and thermopower α, it means that measurements have been performed on single crystals in at least one principal crystallographic direction. The thick solid lines show the situation prevailing until two years ago, while the thick shaded lines indicate the results published during the last two years.

The particular coefficient α_{111} in the expansion

$$\alpha_{11}(B_1) = \alpha^0_{11} + \alpha_{111} B_1 + D_{11} B_1^2 \tag{56}$$

should be equal to zero in the case of diffusion. Since this coefficient was found by Sümengen and Saunders (1972*b*) to be nonzero at 77 and 196 K it might prove that phonon drag exists at higher temperatures than expected. O. P. Hansen (personal communication) has recently found α_{111} to be nonzero at lower temperature.

7. Concluding Remarks

Great strides have been made these last few years in our understanding of the transport properties of the group V semimetals. From an experimental viewpoint, results are now available on well-characterized single crystals, and there is generally good agreement between results published by various groups. Fig. 16 shows that the last two years have seen the extension of the data to ultralow temperatures for the three semimetals. This has brought some new information as well as promises of superconducting behaviour. It may be seen also from Fig. 16 that we now know much more about arsenic, which was the poor relative of the series a couple of years ago.

Thanks to the introduction of new techniques such as dilution refrigeration and squids, careful experiments have led to the separation of the ideal part of the electrical resistivity from the much larger residual component at ultralow temperatures. This has enabled an investigation of the region where small angle electron–phonon scattering was expected to occur.

Thermal conductivity measurements revealed the various mechanisms contributing to heat transport, and eventually regions where one mechanism predominates, thus allowing theoretical predictions to be checked. The knowledge of the electronic component of the thermal conductivity in conjunction with that of the electrical resistivity gave access to the Lorenz number, which was found to be close to the Sommerfeld value at ultralow temperatures, and to deviate appreciably from this value at higher temperatures. In bismuth, high dielectric maxima reaching $100\ \mathrm{W\,cm^{-1}\,K^{-1}}$ were observed in large samples, suggesting that this material constitutes the best heat conductor in the liquid helium range. Also, because of the dramatic q-dependence of the relaxation times of the low energy phonons, their contribution to heat transport could be observed at relatively high temperatures. In addition to their fundamental interest, these observations may contribute to a new approach to low temperature thermoelectric refrigeration, since the lattice thermal conductivity is the sole parameter on which the thermoelectric figure of merit (24) depends, and which can be controlled independently.

Concerning the thermopower, phonon-drag effects have been observed now in the three semimetals, and these have been found to be very sensitive to the size of the samples. The effect of phonon drag on the electrical conductivity might be important in bismuth and to a lesser extent in the two other semimetals. Despite the complexity of electron–phonon interactions in these materials, the group V semimetals are the choice materials for such studies, since they have small densities of degenerate carriers without predominant impurity scattering.

As regards the interpretation of the results, some progress may be noted in the understanding of the scattering mechanisms at low temperatures. Although the odd low temperature variation of the ideal resistivity of the three group V semimetals, as well as the peculiar size effects observed in bismuth, are not yet explained, some models have been proposed and seem to favour the hypothesis of a dominant highly anisotropic electron–phonon scattering.

The diffusion thermopower is quite well understood in arsenic and antimony and the pseudoparabolic model might be the clue to the interpretation of the bismuth data. Although the theory of phonon-drag effects has been extended to the group V semimetals, this theory still needs to be refined and many parameters are still lacking in order to explain the experimental results.

The experimental determination of the drastic temperature variation of the band parameters in bismuth up to room temperature is a fundamental ingredient in the analysis of the higher temperature data. However, quantitative data for one of the masses are still urgently needed. Also the effective mass approximation needs to be questioned when applied to the conduction band of bismuth.

Acknowledgments

The author is much indebted to Professor J-P. Michenaud and Dr C. Uher, Dr J. Heremans and Mr J. Boxus for critical reading of the manuscript and many useful suggestions. He is also grateful to Professor G. A. Saunders and Dr O. P. Hansen for enlightening discussions. The patience of Mrs R. Poncin in typing the manuscript is also greatly appreciated.

Note added in proof

The scattering of phonons by electrons in metals at low temperatures leads to a T^2 variation of the lattice thermal conductivity. This has often been extrapolated to the case of semimetals. However, we (J. Boxus, unpublished data) have recently reexamined the situation and found that it is not obvious at all that the arguments invoked for metals would also apply to the group V semimetals. Thus the discussion in Section 4*b* concerning the T^2 law will probably not be valid when the subject is studied further theoretically.

References

Abeles, B., and Meiboom, S. (1956). *Phys. Rev.* **101**, 544.
Akgöz, Y. C., and Saunders, G. A. (1975*a*). *J. Phys.* C **8**, 1387.
Akgöz, Y. C., and Saunders, G. A. (1975*b*). *J. Phys.* C **8**, 2962.
Aleksandrov, B. N., Dukin, V. V., Maslova, L. A., and Tsivinskii, S. V. (1972). *Sov. Phys. JETP* **34**, 125.
Alers, P. B., and Webber, R. T. (1953). *Phys. Rev.* **91**, 1060.
Anagnostopoulos, K., and Aubrey, J. E. (1976). *J. Phys.* F **6**, L181.
Aubrey, J. E. (1971). *J. Phys.* F **1**, 493.
Aubrey, J. E., and Creasey, C. J. (1969). *J. Phys.* C **2**, 824.
Bansal, S. K., and Duggal, V. P. (1973). *Phys. Status Solidi* (b) **56**, 717.
Bhagat, S. M., and Manchon, D. D. (1967). *Phys. Rev.* **164**, 966.
Blatt, F. J. (1968). 'Physics of Electronic Conduction in Solids' (McGraw-Hill: New York).
Blewer, R. S., and Zebouni, N. H. (1966). *Phys. Lett.* **23**, 297.
Boxus, J., and Issi, J-P. (1977). *J. Phys.* C **10**, L397.
Boyle, W. S., and Smith, G. E. (1963). *In* 'Progress in Semiconductors', Vol. 7 (Ed. A. F. Gibson) (Wiley: New York).
Bressler, M. S., and Red'ko, N. A. (1971). *Zh. Eksp. Teor. Fiz.* **61**, 287; English translation (1972) *Sov. Phys. JETP* **34**, 149.
Brown, R. N., Mavroides, J. G., and Lax, B. (1963). *Phys. Rev.* **129**, 2055.
Bube, H. (1960). 'Photoconductivity of Solids' (Wiley: New York).
Casimir, H. B. G. (1938). *Physica* **5**, 495.
Cheruvier, E., and Hansen, O. P. (1975). *J. Phys.* C **8**, L346.
Chopra, V., Ray, R. K., and Bhagat, S. M. (1971). *Phys. Status Solidi* (a) **4**, 205.
Cohen, M. H. (1961). *Phys. Rev.* **121**, 387.
Drabble, J. R., and Wolfe, R. (1956). *Proc. Phys. Soc. London* B **69**, 1101.
Dresselhaus, M. S. (1971). *J. Phys. Chem. Solids* **32**, Suppl. No. 1, p. 3.
Edelman, V. S. (1976). *Adv. Phys.* **25**, 555.
Ettingshausen, A., and Nernst, W. (1886). *Wied. Ann.* **29**, 343.
Fenton, E. W., Jan, J. P., Kartsson, A., and Singer, R. (1969). *Phys. Rev.* **184**, 663.

Friedman, A. N. (1967). *Phys. Rev.* **159**, 553.
Friedman, A. N., and Koenig, S. H. (1960). *IBM J. Res. Develop.* **4**, 1958.
Gallo, C. F., Chandrasekhar, B. S., and Sutter, P. H. (1963). *J. Appl. Phys.* **34**, 144.
Garcia, N., and Kao, Y. H. (1968). *Phys. Lett.* A **26**, 373.
Goldsmid, H. J. (1964). 'Thermoelectric Refrigeration' (Plenum: New York).
Goodman, B. (1954). Ph.D. Thesis, University of Pennsylvania.
Grüneisen, E., and Gielessen, J. (1936). *Ann. Phys.* (*Liepzig*) **27**, 243.
Hansen, O. P. (1977). *Phys. Status Solidi* **82**, 133.
Hansen, O. P., Cheruvier, E., Michenaud, J-P., and Issi, J-P. (1978). *J. Phys.* C **11**, 1825.
Harman, T. C., and Honig, J. M. (1967). 'Thermoelectric and Thermomagnetic Effects and Applications' (McGraw-Hill: New York).
Hartman, R. (1969). *Phys. Rev.* **181**, 1070.
Heremans, J., and Hansen, O. P. (1979). *J. Phys.* C **12**, 3483.
Heremans, J., Issi, J-P., Rashid, A. A. M., and Saunders, G. A. (1977). *J. Phys.* C **10**, 4511.
Herring, C. (1954*a*). *Phys. Rev.* **95**, 954.
Herring, C. (1954*b*). *Phys. Rev.* **96**, 1163.
Issi, J-P., and Mangez, J. H. (1972). *Phys. Rev.* B **6**, 4429.
Issi, J-P., Michenaud, J-P., and Heremans, J. (1976). Proc. 14th Int. Conf. on Thermal Conductivity, Storrs, Connecticut, p. 127 (Plenum: New York).
Issi, J-P., Michenaud, J-P., Moureau, A., and Coopmans, P. (1971). *J. Phys.* E **4**, 512.
Issi, J-P., and Streydio, J. M. (1967). *Adv. Energy Convers.* **7**, 195.
Jacobson, D. M., and Ertl, M. E. (1972). *J. Phys.* D **5**, 1358.
Jeavons, A. P., and Saunders, G. A. (1969). *Proc. R. Soc. London* A **310**, 415.
Jeavons, A. P., and Saunders, G. A. (1970). *Solid State Commun.* **8**, 995.
Juretschke, H. J. (1955). *Acta Crystallogr.* **8**, 716.
Kane, E. O. (1957). *J. Phys. Chem. Solids* **1**, 249.
Keyes, R. J., Zwerdling, S., Foner, S., Kolm, H. H., and Lax, B. (1956). *Phys. Rev.* **104**, 1804.
Klemens, P. G. (1951). *Proc. Phys. Soc. London* A **64**, 1030.
Kopylov, V. N., and Mezhov-Deglin, L. P. (1974). *Sov. Phys. JETP* **38**, 357.
Korenblit, I. Ya. (1969). *Sov. Phys. Semicond.* **2**, 1192.
Korenblit, I. Ya., Kuznetsov, M. E., Muzhdaba, V. M., and Shalyt, S. S. (1970). *Sov. Phys. JETP* **30**, 1009.
Korenblit, I. Ya., Kuznetsov, M. E., and Shalyt, S. S. (1969). *Sov. Phys. JETP* **29**, 4.
Kukkonen, C. A., and Maldague, P. F. (1976). *J. Phys.* F **6**, L301.
Kukkonen, C. A., and Sohn, K. F. (1977). *J. Phys.* F **7**, L193.
Kuznetsov, N. E., Oskotskii, V. S., Pol'shin, V. I., and Shalyt, S. S. (1970). *Sov. Phys. JETP* **30**, 607.
Kuznetsov, M. E., and Shalyt, S. S. (1967). *JETP Lett.* **6**, 217.
Lax, B., and Mavroides, J. G. (1960). 'Advances in Solid State Physics' (Academic: New York).
Leavens, C. R., and Laubitz, M. J. (1975). *J. Phys.* F **5**, 1519.
Little, N. C. (1926). *Phys. Rev.* **28**, 418.
Mc Clure, J. W., and Choi, K. H. (1977). *Solid State Commun.* **21**, 1015.
Mase, S., Von Molnar, S., and Lawson, A. W. (1962). *Phys. Rev.* **127**, 1030.
Michenaud, J-P., Cheruvier, E., and Issi, J-P. (1971). *Solid State Commun.* **9**, 1433.
Michenaud, J-P., and Issi, J-P. (1972). *J. Phys.* C **5**, 3061.
Michenaud, J-P., Streydio, J. M., Issi, J-P., and Luyckx, A. (1970). *Solid State Commun.* **8**, 455.
Okada, J. (1957). *J. Phys. Soc. Jpn* **12**, 1327.
Oktü, O., and Saunders, G. A. (1967*a*). *Proc. Phys. Soc. London* **91**, 156.
Oktü, O., and Saunders, G. A. (1967*b*). *Phys. Lett.* A **25**, 266.
Parrott, J. E. (1957). *Proc. Phys. Soc. London* B **70**, 590.
Pratt, W. P., and Uher, C. (1978). *Phys. Lett.* A **68**, 74.
Ravich, Yu. I., Efimova, B. A., and Tamarchenko, V. I. (1971). *Phys. Status Solidi* (b) **43**, 11, 453.
Red'ko, N. A., Bresler, M. S., and Shalyt, S. S. (1970). *Sov. Phys. Solid State* **11**, 2435.
Red'ko, N. A., and Shalyt, S. S. (1968). *Sov. Phys. Solid State* **10**, 1233.
Rosenberg, H. M. (1955). *Philos. Trans. R. Soc. London* **247**, 441.
Saunders, G. A., and Oktü, O. (1968). *J. Phys. Chem. Solids* **29**, 327.
Saunders, G. A., and Sümengen, Z. (1972). *J. Phys.* F **2**, 972.
Shalyt, S. S. (1944). *J. Phys. USSR* **8**, 315.

Smith, G. E., and Wolfe, R. (1966). *J. Phys. Soc. Jpn* **21**, 651.
Sondheimer, E. H. (1952). *Proc. Phys. Soc. London* A **65**, 561.
Steele, M. C., and Babiskin, J. (1955). *Phys. Rev.* **98**, 359.
Sümengen, Z., and Saunders, G. A. (1972*a*). *J. Phys.* C **5**, 425.
Sümengen, Z., and Saunders, G. A. (1972*b*). *Solid State Commun.* **10**, 37.
Sümengen, Z., Turetken, N., and Saunders, G. A. (1974). *J. Phys.* C **7**, 2204.
Tanaka, K., Suri, S. K., and Jain, A. L. (1968). *Phys. Rev.* **170**, 664.
Tanuma, S., Farag, B. S., Inada, R., and Sugihara, K. (1969). Proc. Soviet–Japanese Conf. on Low Temperature Physics, Novosibirsk, U.S.S.R.
Uher, C. (1975). *Phys. Status Solidi* (b) **70**, 219.
Uher, C. (1978*a*). *J. Phys.* (*Paris*) *Colloq.* C **6**, Suppl. No. 8, p. 1054.
Uher, C. (1978*b*). *J. Phys.* F **8**, 2559.
Uher, C., and Goldsmid, H. J. (1974*a*). *Phys. Status Solidi* (b) **63**, 163.
Uher, C., and Goldsmid, H. J. (1974*b*). *Phys. Status Solidi* (b) **65**, 765.
Uher, C., and Opsal, J. L. (1978). *Phys. Rev. Lett.* **40**, 1518.
Uher, C., and Pratt, W. P. (1977). *Phys. Rev. Lett.* **39**, 491.
Uher, C., and Pratt, W. P. (1978). *J. Phys.* F **8**, 1979.
Vecchi, M. P., and Dresselhaus, M. S. (1974). *Phys. Rev.* B **10**, 771.
White, G. K., and Woods, S. B. (1958). *Philos. Mag.* **3**, 342.
Zawadzki, W. (1974). *Adv. Phys.* **23**, 435.
Zawadzki, W., and Szymanska, W. (1971). *Phys. Status Solidi* (b) **45**, 415.
Zitter, R. N. (1962). *Phys. Rev.* **127**, 1471.

Manuscript received 6 June 1979